Gastroenterology 2017;153:1320–1337

# Circulating and Tissue-Resident CD4$^+$ T Cells With Reactivity to Intestinal Microbiota Are Abundant in Healthy Individuals and Function Is Altered During Inflammation

**Ahmed N. Hegazy**,[1,2,*] **Nathaniel R. West**,[1,2,*] Michael J. T. Stubbington,[3,4] Emily Wendt,[1] Kim I. M. Suijker,[2] Angeliki Datsi,[1] Sebastien This,[1] Camille Danne,[2] Suzanne Campion,[5] Sylvia H. Duncan,[6] Benjamin M. J. Owens,[1] Holm H. Uhlig,[1,7] Andrew McMichael,[5] Oxford IBD Cohort Investigators, Andreas Bergthaler,[8] Sarah A. Teichmann,[3,4] Satish Keshav,[1] and Fiona Powrie[1,2]

*[1]Translational Gastroenterology Unit, Nuffield Department of Clinical Medicine, Experimental Medicine Division, John Radcliffe Hospital, University of Oxford, United Kingdom; [2]Kennedy Institute of Rheumatology, Nuffield Department of Orthopaedics, Rheumatology and Musculoskeletal Sciences, University of Oxford, United Kingdom; [3]European Molecular Biology Laboratory-European Bioinformatics Institute, Hinxton, United Kingdom; [4]Wellcome Trust Sanger Institute, Wellcome Trust Genome Campus, Hinxton, Cambridge, United Kingdom; [5]Nuffield Department of Medicine Research Building, University of Oxford, Oxford, United Kingdom; [6]Microbial Ecology Group, Rowett Institute of Nutrition and Health, University of Aberdeen, Aberdeen, United Kingdom; [7]Department of Paediatrics, University of Oxford, Oxford, United Kingdom; and [8]CeMM Research Center for Molecular Medicine of the Austrian Academy of Sciences, Vienna, Austria*

**See Covering the Cover synopsis on page 1175.**



**BACKGROUND & AIMS:** Interactions between commensal microbes and the immune system are tightly regulated and maintain intestinal homeostasis, but little is known about these interactions in humans. We investigated responses of human CD4$^+$ T cells to the intestinal microbiota. We measured the abundance of T cells in circulation and intestinal tissues that respond to intestinal microbes and determined their clonal diversity. We also assessed their functional phenotypes and effects on intestinal resident cell populations, and studied alterations in microbe-reactive T cells in patients with chronic intestinal inflammation. **METHODS:** We collected samples of peripheral blood mononuclear cells and intestinal tissues from healthy individuals (controls, n = 13−30) and patients with inflammatory bowel diseases (n = 119; 59 with ulcerative colitis and 60 with Crohn's disease). We used 2 independent assays (CD154 detection and carboxy-fluorescein succinimidyl ester dilution assays) and 9 intestinal bacterial species (*Escherichia coli, Lactobacillus acidophilus, Bifidobacterium animalis* subsp *lactis, Faecalibacterium prausnitzii, Bacteroides vulgatus, Roseburia intestinalis, Ruminococcus obeum, Salmonella typhimurium,* and *Clostridium difficile*) to quantify, expand, and characterize microbe-reactive CD4$^+$ T cells. We sequenced T-cell receptor V$\beta$ genes in expanded microbe-reactive T-cell lines to determine their clonal diversity. We examined the effects of microbe-reactive CD4$^+$ T cells on intestinal stromal and epithelial cell lines. Cytokines, chemokines, and gene expression patterns were measured by flow cytometry and quantitative polymerase chain reaction. **RESULTS:** Circulating and gut-resident CD4$^+$ T cells from controls responded to bacteria at frequencies of 40−4000 per million for each bacterial species tested. Microbiota-reactive CD4$^+$ T cells were mainly of a memory phenotype, present in peripheral blood mononuclear cells and intestinal tissue, and had a diverse T-cell receptor V$\beta$ repertoire. These cells were functionally heterogeneous, produced barrier-protective cytokines, and stimulated intestinal stromal and epithelial cells via interleukin 17A, interferon gamma, and tumor necrosis factor. In patients with inflammatory bowel diseases, microbiota-reactive CD4$^+$ T cells were reduced in the blood compared with intestine; T-cell responses that we detected had an increased frequency of interleukin 17A production compared with responses of T cells from blood or intestinal tissues of controls. **CONCLUSIONS:** In an analysis of peripheral blood mononuclear cells and intestinal tissues from patients with inflammatory bowel diseases vs controls, we found that reactivity to intestinal bacteria is a normal property of the human CD4$^+$ T-cell repertoire, and does not necessarily indicate disrupted interactions between immune cells and the commensal microbiota. T-cell responses to commensals might support intestinal homeostasis, by producing barrier-protective cytokines and providing a large pool of T cells that react to pathogens.

*Keywords:* Immune Regulation; Microbiota; Cytokines; Tissue-resident Memory T cells.

*Authors share co-first authorship.

***Abbreviations used in this paper:*** **CFSE, carboxy-fluorescein succinimidyl ester; IBD, inflammatory bowel disease; ICOS, inducible T-cell costimulator; IFN, interferon; IL, interleukin; LPMC, Lamina propria mononuclear cell; PBMC, peripheral blood mononuclear cell; SEB, *Staphylococcus* enterotoxin B; TCR, T-cell receptor; Th, T helper; TNF, tumor necrosis factor.**

**Most current article**



0016-5085
https://doi.org/10.1053/j.gastro.2017.07.047

**EDITOR'S NOTES**

BACKGROUND AND CONTEXT

$CD4^+$ T cell responses to intestinal bacteria are known to occur, however these responses remain poorly characterized in humans.

NEW FINDINGS

Microbiota-reactive $CD4^+$ T cells are prevalent and normal constituents of the human immune system that are functionally altered during IBD pathogenesis.

LIMITATIONS

The functional relevance of the detected T-cell responses in humans remains to be elucidated.

IMPACT

T-cell responses to commensals might support intestinal homeostasis by producing barrier-protective cytokines and providing a large pool of T cells with potential cross-reactivity to pathogens.

Vast numbers of microbes populate the gastrointestinal tract and contribute to digestion, epithelial barrier integrity, and development of appropriately educated mucosal immunity.[1] Intestinal immune responses are tightly regulated to allow protective immunity against pathogens, while limiting responses to dietary antigens and innocuous microbes. The "mucosal firewall" prevents systemic dissemination of microbes by confining microbial antigens to the gut-associated lymphoid tissue.[2] In the gut-associated lymphoid tissue, dendritic cells drive regulatory T-cell differentiation in response to dietary antigens and commensal bacteria.[3] Nevertheless, vast numbers of potentially commensal-reactive effector and memory T cells populate intestinal mucosae.[4] Recent evidence suggests that in mice, tolerance to commensal-derived antigens may be lost during pathogen-induced epithelial damage and subsequent transient exposure to commensals.[1,5] In humans, circulating memory T cells recognize peptides derived from gut bacteria and can cross-react to pathogens, which can confer immunologic advantage during subsequent new infections.[6,7] Although this process can be beneficial during homeostasis, deranged responses to commensals may promote inflammatory conditions, such as inflammatory bowel diseases (IBDs).

IBDs (including Crohn's disease and ulcerative colitis) result from a prolonged disturbance of gut homeostasis, the precise etiology of which is uncertain. One hypothesis is that, in genetically susceptible individuals, IBD may be triggered by intestinal dysbiosis that promotes aberrant immune stimulation.[8] Indeed, in mouse models of colitis, intestinal microbiota promote inflammation in part by stimulating microbiota-reactive $CD4^+$ T cells.[5,9] Whether this drives IBD in humans, however, remains unknown.

Although $CD4^+$ T-cell responses to intestinal bacteria are known to occur in humans,[10–12] several aspects of this topic are largely uncharacterized, including the frequency of human T cells in the gut and periphery that are reactive to phylogenetically distinct intestinal microbes; the T-cell receptor (TCR) diversity and clonotype sharing of these T cells; the functional phenotype of gut microbe-reactive T cells and their impact on tissue-resident cell populations; and how microbe-reactive T cells change during chronic intestinal inflammation. To address this knowledge gap, we extensively characterized $CD4^+$ T-cell responses to intestinal microbiota in healthy individuals and IBD patients.

Using 2 independent assays, we observed that for almost all enteric bacteria examined, bacteria-reactive $CD4^+$ T cells were present at a frequency of 40−500 per million $CD4^+$ T cells in adult peripheral blood. Bacteria-reactive T cells were also prevalent in the gut mucosa, with prominent enrichment for proteobacteria reactivity. Microbiota-responsive T cells showed a diverse TCR V$\beta$ repertoire and potently stimulated inflammatory responses by intestinal epithelial and stromal cells. Intriguingly, T cells from IBD patients displayed a normal spectrum of microbial responses, but expressed high amounts of interleukin (IL) 17A, consistent with increased amounts of T-helper (Th) 17-polarizing cytokines in inflamed intestinal tissue. Collectively, these data demonstrate that microbiota-reactive $CD4^+$ T cells are prevalent and normal constituents of the human immune system that are functionally altered during IBD pathogenesis.

## Materials and Methods

### *Human Samples and Cell Isolation*

Leukoreduction chambers from healthy individuals were obtained from the National Blood Service (Bristol, UK). Peripheral EDTA blood samples were obtained from IBD patients attending the John Radcliffe Hospital Gastroenterology unit or from healthy in-house volunteers. IBD patients (n = 119; ulcerative colitis, n = 59; Crohn's disease, n = 60) diagnosed by endoscopic, histologic, and radiologic criteria were recruited for the study. Healthy volunteers (n = 30) without any known underlying acute or chronic pathologic condition served as control donors. All donors provided informed written consent. The National Health Service Research Ethics System provided ethical approval (reference numbers 09/H0606/5 for IBD patients and 11/YH/0020 for controls; OCHRe ref 15/A237 for cord blood samples). For details regarding cell isolation, see Supplementary Experimental Procedures.

### *CD154-Based Detection of Antigen-Specific T Cells*

CD154 detection was done as described previously.[13,14] Briefly, cells were plated at $5 \times 10^6/cm^2$ for 7−12 hours with heat-inactivated bacteria. Brefeldin A (5 $\mu$g/mL; Sigma Aldrich, St Louis, MO) was added at 2 hours. After 8−12 hours, cells were harvested and treated as described in the section on intracellular cytokine, CD154, and transcription factor staining. For magnetic cell separation enrichment of $CD4^+CD154^+$ T cells, see Supplementary Experimental Procedures.

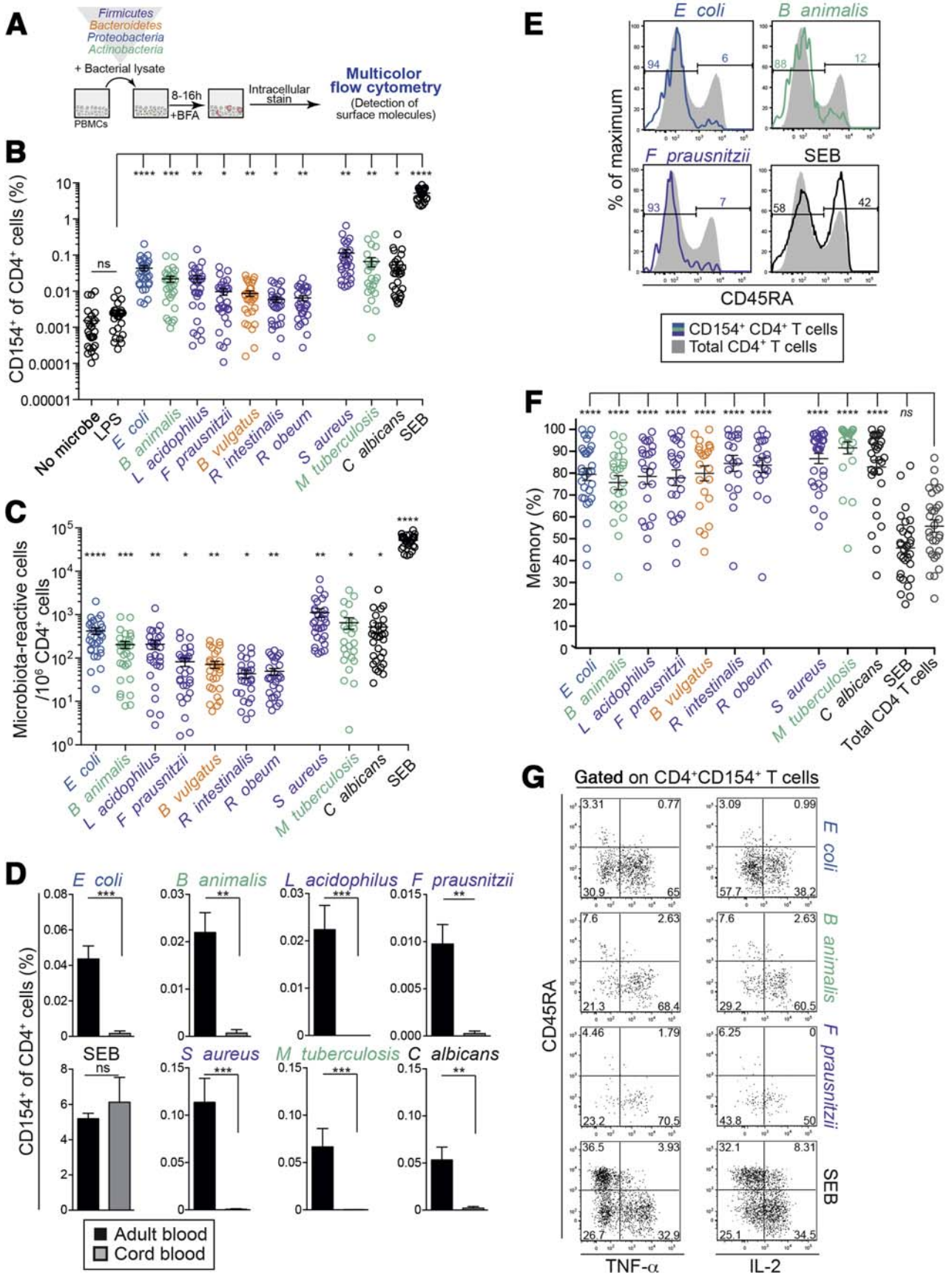
A
Firmicutes
Bacteroidetes
Proteobacteria
Actinobacteria
+ Bacterial lysate
PBMCs
8-16h
+BFA
Intracellular stain
Multicolor flow cytometry
(Detection of surface molecules)
B
CD154+ of CD4+ cells (%)
ns
No microbe
LPS
E coli
B animalis
L acidophilus
F prausnitzii
B vulgatus
R intestinalis
R obeum
S aureus
M tuberculosis
C albicans
SEB
C
Microbiota-reactive cells /10^6 CD4+ cells
D
E coli
B animalis
L acidophilus
F prausnitzii
SEB
S aureus
M tuberculosis
C albicans
CD154+ of CD4+ cells (%)
Adult blood
Cord blood
E
E coli
B animalis
F prausnitzii
SEB
% of maximum
CD45RA
CD154+ CD4+ T cells
Total CD4+ T cells
F
Memory (%)
Total CD4 T cells
G
Gated on CD4+CD154+ T cells
CD45RA
TNF-α
IL-2

### Antigen-Specific Recall Response (Carboxy-Fluorescein Succinimidyl Ester Dilution Assay) and T-Cell Culture

Memory $CD4^+$ $CD45RO^+$ $CD45RA^-$ T cells were enriched from peripheral blood mononuclear cells (PBMCs) with untouched memory $CD4^+$ T cell enrichment kit (Miltenyi Biotec, Bergisch Gladbach, Germany), sorted to >97% purity on a FACS ARIA III (BD, San Jose, CA) using CD45RA and CD45RO expression, and were labeled with carboxyfluorescein succinimidyl ester (CFSE) or violet proliferation dye (Invitrogen, Carlsbad, CA). $CD14^+$ monocytes were isolated from PBMC using anti-CD14 microbeads (Miltenyi Biotec), irradiated (45 Gy) and then pre-incubated for 3 hours with bacterial lysates before T-cell co-culture. T cells were co-cultured with the irradiated autologous monocytes at a ratio of 2:1 for 5−7 days. Cells were cultured in RPMI-1640 supplemented with 2 mM glutamine, 1% (v/v) non-essential amino acids, 1% (v/v) sodium pyruvate, penicillin (50 U/mL), streptomycin (50 mg/mL; all from Invitrogen), and 5% (v/v) human serum (National Blood Service, Bristol, UK). $CD14^+$ monocytes were irradiated (45 Gy) and then pre-incubated for 3 hours with bacterial lysates before T-cell co-culture. For major histocompatibility complex II blockade, 10 $\mu$g/mL of a pan-HLA class-II blocking antibody (HLA-DR, DP, DQ [Tü39]) was added 30 minutes before T-cell co-culture. T-cell lines were generated by sorting $CFSE^{low}$ inducible T-cell costimulator $(ICOS)^{high}$ $CD4^+$ T cells after 7 days of stimulation and expanding them with IL2 (300 U/mL) and anti-CD3/CD28 beads (beads/T cell ratio, 1:4, Dynals) for 10−14 days. Supernatants were collected from $1 \times 10^6$ $CD4^+$ T cells stimulated for 24 hours with phorbol myristate acetate (5 ng/mL) and ionomycin (500 ng/mL; Sigma).

### Flow Cytometry and Cell Sorting

PBMCs and lamina propria mononuclear cells were stained according to standard protocols. For details, see Supplementary Experimental Procedures.

### Intracellular Cytokine, CD154, and Transcription Factor Staining

For intracellular cytokine staining, cells were stained with fixable viability dye eFluor 780 (eBioscience, San Diego, CA) and surface markers, fixed with 2% formaldehyde (Merck, Kenilworth, NJ), and stained for cytokines in magnetic cell separation buffer containing 0.05% saponin (Sigma-Aldrich). Transcription factor expression was analyzed using the FoxP3 staining buffer set (eBioscience) according to manufacturer's instructions.

### Stimulation of Intestinal Cell Lines

CCD18Co (non-transformed human colon fibroblasts; ATCC, Manassas, VA), and LIM1863 (human colon epithelial cells; a kind gift of Dr Robert Whitehead, Ludwig Institute for Cancer Research) cells were cultured in humidified incubators with 5% $CO_2$ at 37°C in Dulbecco's modified Eagle medium or RPMI media (Sigma) with 10% fetal calf serum (Sigma) and 100 U penicillin/0.1 mg/mL streptomycin. Cells were stimulated with 5% T-cell supernatants for 24 hours. Cytokine neutralization was achieved by supernatant pre-incubation for 1−2 hours with 10 $\mu$g/mL anti−IL17A (eBio64CAP17), anti−interferon (IFN) gamma (B27), anti−tumor necrosis factor (TNF)−$\alpha$ (Remicade; Janssen Biotech, Horsham, PA), and anti−IL22 (IL22JOP).

### Statistics

Statistical analyses were performed with GraphPad Prism, version 6.0 for Macintosh (GraphPad Software, La Jolla, CA). Statistically significant $P$ values were indicated as follows: NS, not significant; *$P \leq .05$; **$P \leq .01$; ***$P \leq .001$; ****$P \leq .0001$. Tests are specified in figure legends.

## Results

### Healthy Adults Possess Circulating Memory $CD4^+$ T Cells That Are Reactive to Intestinal Microbiota

CD154 (also known as CD40 ligand) is rapidly up-regulated by $CD4^+$ T cells after antigen stimulation, irrespective of their differentiation phenotype, major histocompatibility complex alleles, or the precise nature of the antigenic epitope.[13,14] We therefore used CD154 to detect naïve and memory $CD4^+$ T-cell responses among PBMCs after stimulation with heat-inactivated bacteria (Figure 1*A*). Seven aerobic and anaerobic intestinal bacterial species representing the 4 dominant gut phyla were chosen: *Escherichia coli*, *Lactobacillus acidophilus*, *Bifidobacterium animalis subsp. lactis*, *Faecalibacterium prausnitzii*,



**Figure 1.** Healthy adults possess circulating memory $CD4^+$ T cells that are reactive to intestinal microbiota. PBMCs were stimulated with heat-inactivated bacteria for 8−12 hours, and bacteria-reactive $CD4^+$ T cells were detected by intracellular CD154 expression. (*A*) Experimental setup. (*B*) $CD154^+$ frequencies among peripheral $CD4^+$ T cells in adults after short-term stimulation with heat-inactivated bacteria (n = 30 independent donors). (*C*) Estimated microbiota-reactive cells per million $CD4^+$ T cells in adult blood (n = 30). The numbers of microbiota-reactive T cells were calculated based on the frequencies of $CD4^+CD154^+$ T cells. Background (no microbe stimulation) was subtracted from bacterial stimulations. Significance calculated in relation to lipopolysaccharide stimulation. (*D*) Frequencies (±SEM) of $CD154^+$ cells among $CD4^+$ T cells in adult (n = 30) or cord blood (n = 3) after short-term stimulation with heat-inactivated bacteria. (*E*) Expression of CD45RA on $CD4^+CD154^+$ T cells, showing 4 representative stimulations of the same donor. (*F*) Mean (±SEM) frequencies of memory cells within $CD4^+CD154^+$ T cells. Each symbol represents an antigen-reactive population from one individual (n = 19−30). (*G*) Expression of CD45RA, TNF-$\alpha$, and IL2 by $CD4^+CD154^+$ T cells after short-term PBMC stimulation with bacterial lysates. Statistics: (*B*, *C*, *F*) 1-way analysis of variance with Sidak's multiple comparison test; (*D*) Mann-Whitney test.

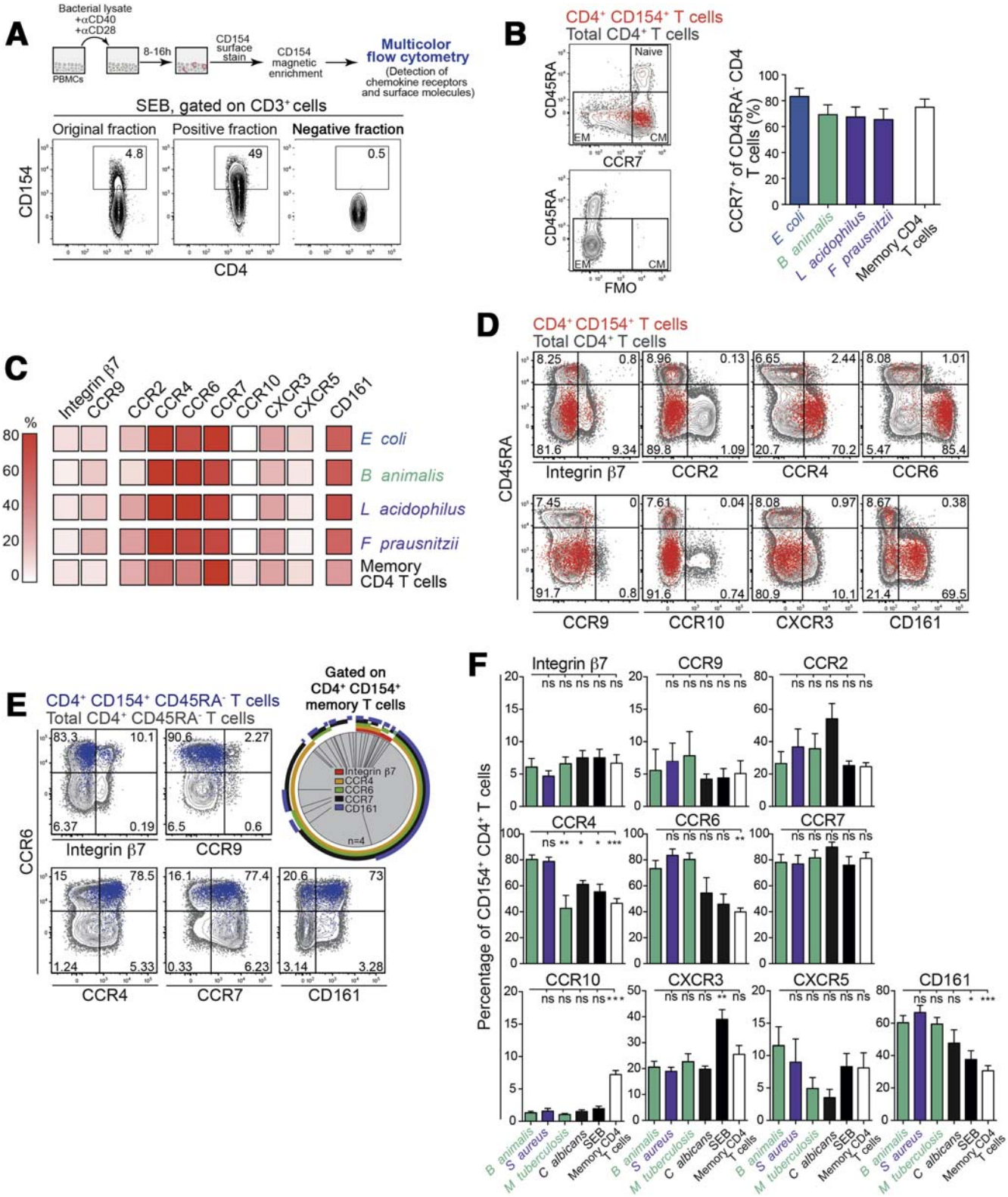
A
Bacterial lysate
+αCD40
+αCD28
PBMCs
8-16h
CD154 surface stain
CD154 magnetic enrichment
Multicolor flow cytometry
(Detection of chemokine receptors and surface molecules)
SEB, gated on CD3+ cells
Original fraction
Positive fraction
Negative fraction
CD154
CD4
4.8
49
0.5
B
CD4+ CD154+ T cells
Total CD4+ T cells
CD45RA
CCR7
Naive
EM
CM
FMO
CCR7+ of CD45RA- CD4 T cells (%)
E. coli
B. animalis
L. acidophilus
F. prausnitzii
Memory CD4 T cells
C
Integrin β7
CCR9
CCR2
CCR4
CCR6
CCR7
CCR10
CXCR3
CXCR5
CD161
%
E. coli
B. animalis
L. acidophilus
F. prausnitzii
Memory CD4 T cells
D
CD4+ CD154+ T cells
Total CD4+ T cells
CD45RA
Integrin β7
CCR2
CCR4
CCR6
CCR9
CCR10
CXCR3
CD161
E
CD4+ CD154+ CD45RA- T cells
Total CD4+ CD45RA- T cells
Gated on CD4+ CD154+ memory T cells
CCR6
Integrin β7
CCR9
CCR4
CCR7
CD161
n=4
F
Percentage of CD154+ CD4+ T cells
Integrin β7
CCR9
CCR2
CCR4
CCR6
CCR7
CCR10
CXCR3
CXCR5
CD161
B. animalis
S. aureus
M. tuberculosis
C. albicans
SEB
Memory CD4 T cells

*Bacteroides vulgatus*, *Roseburia intestinalis*, and *Ruminococcus obeum* (Supplementary Figure 1*A* and Supplementary Table 1). These bacteria are common in the healthy intestine, but are altered in relative abundance during inflammation.[15,16] Furthermore, we analyzed responses to *Salmonella typhimurium* and *Clostridium difficile* due to their association with IBD.[17,18] T-cell responses to these bacteria were compared with those against well-characterized barrier surface-related microbes that drive robust Th17 responses (*Staphylococcus aureus* and *Candida albicans*) or strong Th1 responses (*Mycobacterium tuberculosis*).[19,20] The presence of a large pool of *M tuberculosis*-reactive memory Th1 cells in non-exposed individuals has been documented previously. The responses in healthy controls are directed toward non-tuberculous mycobacteria rather than toward *M tuberculosis*.[19,21,22] The superantigen *Staphylococcus* enterotoxin B (SEB) was used as a positive stimulation control.

Stimulation with enteric bacteria reproducibly induced detectable numbers of $CD4^+CD154^+$ T cells in the peripheral blood. $CD4^+$ T cells reactive to *S aureus*, *C albicans*, and *M tuberculosis* were generally more abundant (Figure 1*B* and Supplementary Figure 1*B* and *C*).

Activation markers CD69 and ICOS were up-regulated on activated antigen-reactive $CD4^+CD154^+$ T cells (Supplementary Figure 1*D*). Responses were major histocompatibility complex II–dependent (Supplementary Figure 1*E*), and lipopolysaccharide failed to induce CD154 expression, confirming that CD154 up-regulation was not a consequence of non-specific microbial responses (Figure 1*B* and Supplementary Figure 1*C*). Based on $CD154^+$ cell frequencies, we calculated that enteric bacteria-reactive $CD4^+$ T cells were present at precursor frequencies of 40–500 cells per $10^6$ circulating $CD4^+$ T cells for almost all enteric bacteria surveyed (Figure 1*C* and Supplementary Figure 1*F*).

The newborn gut is primarily colonized with maternal vaginal and fecal bacteria after birth.[23] To understand whether T-cell reactivity to microbes develops after birth, we compared CD154 expression in umbilical cord blood with adult blood after enteric bacteria stimulation. As expected, appreciable responses to microbiota were observed only in adult blood. However, $CD4^+CD154^+$ T-cell frequencies after SEB stimulation were similar between adult and cord blood (Figure 1*D* and Supplementary Figure 1*G*).

Human memory T cells down-regulate the naïve marker CD45RA and produce cytokines more efficiently than naïve T cells.[24,25] In healthy individuals, the majority of bacteria-reactive $CD4^+$ T cells had a memory phenotype (>80%, on average), indicating that they had been primed in vivo (Figure 1*E* and *F* and Supplementary Figure 2*A* and *B*). Microbiota-reactive $CD4^+CD154^+CD45RA^-$ T cells expressed high amounts of TNF-$\alpha$ and IL2 when compared to $CD4^+CD154^+CD45RA^+$ T cells (Figure 1*G* and Supplementary Figure 2*C*). Therefore, the circulating pool of memory $CD4^+$ T cells contains numerous microbiota-reactive cells that arise after birth and produce cytokines, including TNF-$\alpha$ and IL2.

## Circulating Microbiota-Reactive $CD4^+$ T Cells Express Surface Molecules That Permit Mucosal Trafficking

Memory T cells express numerous adhesion molecules and chemokine receptors to access different tissues under steady-state and inflammatory conditions.[4,26,27] For example, $\alpha4\beta7$ integrin and chemokine receptor (CCR) 9 regulate T-cell migration to distinct parts of the gut. Blockade of $\alpha4\beta7$ integrin has shown clinical efficacy for treating IBD, whereas CCR9 blockade yielded mixed results.[28,29] To identify homing receptors expressed by bacteria-reactive $CD4^+$ T cells, we enriched $CD4^+CD154^+$ T cells using magnetic beads to visualize rare enteric-bacteria-reactive T cells, and analyzed them by flow cytometry (Figure 2*A*). Microbiota-reactive T cells had a central memory phenotype, with >60% expressing high levels of CCR7 (Figure 2*B*). Furthermore, 5%–10% of $CD4^+CD154^+$ T cells expressed the gut-homing surface markers integrin $\beta7$ and CCR9 (Figure 2*C* and *D*). Relative to total memory $CD4^+$ T cells and $CD4^+CD154^-$ T cells, enteric bacteria-reactive T cells had high expression of the mucosa-homing receptors CCR4 and CCR6 (>60%), low expression of CCR10, and comparable expression of CXCR3 and CCR2 (Figure 2*D* and Supplementary Figure 2*D*). Microbiota-reactive $CD4^+$ T cells also



**Figure 2.** Circulating microbiota-reactive $CD4^+$ T cells express several surface molecules that promote mucosal trafficking. $CD4^+CD154^+$ T cells were analyzed by flow cytometry after magnetic enrichment following short-term PBMC stimulation with heat-inactivated bacteria. (*A*) Experimental setup and enrichment efficiency after stimulation with SEB. (*B*) Representative CD45RA and CCR7 expression on enriched $CD4^+CD154^+$ T cells. Central memory T-cell frequencies are shown (*right bar graph*). Frequencies (±SEM) of 4 independent experiments are depicted with n = 8 independent donors. (*C*) *Heat map* depicting mean frequencies of surface marker and chemokine receptor expression on enriched $CD4^+CD154^+$ T cells (n = 5–8 independent donors). (*D*) Surface marker and chemokine receptor expression frequencies among $CD4^+CD154^+$ T cells after short-term stimulation with *B animalis*. Data representative of 5–8 independent donors. (*E*) Co-expression of surface molecules with CCR6 after short-term stimulation of $CD4^+CD154^+$ $CD45RA^-$ T cells with *B animalis* (*left panel*). Boolean gating analysis shows each possible combination of CCR7, CCR4, CCR6, and CD161 expression (*right panel*). (*F*) Surface marker and chemokine receptor expression frequencies among total memory $CD4^+$ T cells and $CD4^+CD154^+$ T cells after short-term stimulation with *B animalis*, *S aureus*, *M tuberculosis*, *C albicans*, or SEB. Frequencies (±SEM) of 4 independent experiments are depicted with n = 5–8 independent donors. Statistics: (*F*) 1-way analysis of variance with Sidak's multiple comparison test.

expressed high amounts of CD161, a marker enriched on Th17 cells (Figure 2*D* and *E*). The majority of memory $CD4^+CD154^+$ T cells co-expressed CCR7, CCR4, CD161, and CCR6 in various combinations, some of which also expressed integrin $\beta7$ (Figure 2*E, pie chart*). Therefore, circulating microbiota-reactive $CD4^+$ T cells are equipped with several homing receptors that promote mucosal access.

When comparing gut microbiota-reactive $CD4^+$ T cells with those reactive to non-enteric organisms (including *S aureus*, *M tuberculosis*, and *C albicans*), enteric bacteria-reactive T cells were partially enriched only in CCR4 expression (Figure 2*F*). The homing receptor phenotype of enteric bacteria-reactive T cells is consistent with that of T cells reactive to a broad diversity of microbes located at barrier surfaces.

## Microbiota-Reactive $CD4^+$ T Cells Are Enriched in Gut Tissue

The gut harbors $>3 \times 10^{10}$ $CD4^+$ T cells, but their specificity is unknown.[4,5] We therefore estimated the abundance of human microbiota-reactive $CD4^+$ T cells in the gut by examining non-inflamed colon specimens using the CD154 assay (Figure 3*A*). Lamina propria $CD4^+$ T cells showed a dominant effector memory and central memory phenotype and expressed both tissue-resident and gut-related markers, with 80% of cells being $CD69^+$ (Supplementary Figure 3*A*).

We next stimulated lamina propria mononuclear cells with microbial lysates or SEB. We combined intracellular CD154 detection with TNF-$\alpha$ staining to increase assay sensitivity, as lamina propria $CD4^+$ T cells expressed low amounts of CD154 without stimulation (Supplementary Figure 3*B* and *C*). Compared with peripheral blood frequencies of unrelated donors, there were similar frequencies of *S aureus* and SEB reactivity, and reduced *M tuberculosis*-reactivity in the gut. However, gut $CD4^+$ T cells were enriched in reactivity toward intestinal bacteria and *C albicans* (Figure 3*B* and Supplementary Figure 3*D*). Bacteria-reactive cells comprised 150−4000 cells per $10^6$ gut-resident memory $CD4^+$ T cells for all enteric bacteria tested. Given that peripheral blood contained 40−500 bacteria-reactive cells per $10^6$ memory $CD4^+$ T cells (for each bacteria tested), this suggests that bacteria-reactive T cells are 3- to 8-fold more frequent in gut tissue as compared with those in circulation. The strong enrichment of *S typhimurium* and *E coli* reactivity in the gut was confirmed by assessing CD154 and TNF-$\alpha$ expression in $CD4^+$ T cells from donor-matched blood and intestinal tissue (Figure 3*C*). Because the gut harbors up to $3 \times 10^{10}$ memory T cells (vs $5-10 \times 10^9$ in blood),[4] many of which are bacteria-reactive, the absolute number of gut-resident microbiota-reactive $CD4^+$ T cells is likely to be at least 10 times greater than that in peripheral blood.

Gut-resident bacteria-reactive ($CD154^+TNF\text{-}\alpha^+$) T cells produced high amounts of IFN-gamma, IL17A, and IL2, while production of IL22, granulocyte macrophage colony-stimulating factor, and IL4 was generally low (Figure 3*D* and Supplementary Figure 3*E* and *F*). Interestingly, lamina propria T cells showed increased IL17A expression and reduced IFN-gamma production relative to cells with similar reactivity in peripheral blood (Figure 3*D* and Supplementary Figure 3*E*).

## Enteric Bacteria-Reactive $CD4^+$ T Cells Are Clonally Diverse

To assess the clonal diversity of circulating bacteria-reactive memory $CD4^+$ T cells, we expanded CFSE-labeled $CD4^+$ T cells using whole bacteria and autologous irradiated monocytes as antigen presenting cells (Supplementary Figure 4*A*).[20] *S aureus*-, *M tuberculosis*-, and SEB-reactive T cells served as controls. Antigen-reactive T cells proliferated in a major histocompatibility complex II−dependent manner and were readily detectible after 3−6 days (Figure 4*A* and Supplementary Figure 4*B*−*D*). Proliferating cells expressed several activation markers including ICOS, CD25, and OX40 (Figure 4*A* and Supplementary Figure 4*B*, *E*, and *F*). Consistent with the CD154 assay, *S aureus*, *M tuberculosis*, and SEB strongly induced T-cell proliferation (Figure 4*A* and *B* and Supplementary Figure 3*B* and *C*).

Flow cytometry analysis revealed a diverse TCR V$\beta$ repertoire in bacteria-reactive T cells, similar to polyclonal stimulation with phytohemagglutinin but different to stimulation with SEB, which is known to activate a restricted V$\beta$ repertoire (Figure 4*C*).[30] To directly assess the clonal diversity of bacteria-reactive $CD4^+$ T cells, we isolated $CFSE^{low}$ bacteria-reactive memory T cells and assessed TCR V$\beta$ clonotypes by multiplex polymerase chain reaction and deep sequencing. One hundred and fifty to eight hundred clonotypes were detected for each reactivity (Supplementary Figure 4*G*). The largest clonal diversity was detected among *E coli*- and *S typhimurium*−reactive cells, consistent with frequencies observed in the CD154 assay (see Figure 1*B* and *C* and Supplementary Figure 1*B* and *F*). While closely related species (eg, *E coli* vs *S typhimurium*) had 3%−8% overlap in T-cell clonotypes, little clonotype sharing was observed between T cells reactive to more distantly related bacteria (Supplementary Figure 3*H*). Indeed, *E coli*- and *B animalis*−reactive $CD4^+$ T-cell lines were strongly restimulated when cultured with autologous monocytes loaded with *E coli* or *B animalis* lysates, respectively. In contrast, *E coli*−reactive T cells responded weakly to the closely related *S typhimurium*, while *B animalis*−reactive T cells responded weakly to *L acidophilus*, *F prausnitzii*, and *C difficile* (Supplementary Figure 5*A*). These data confirm the low degree of cross-reactivity predicted from TCR V$\beta$ sequencing.

## Microbiota-Reactive Memory $CD4^+$ T Cells Are Functionally Heterogeneous and Produce Barrier-Promoting Cytokines

To functionally characterize circulating microbiota-reactive memory cells, we analyzed $CFSE^{low}$ cells using

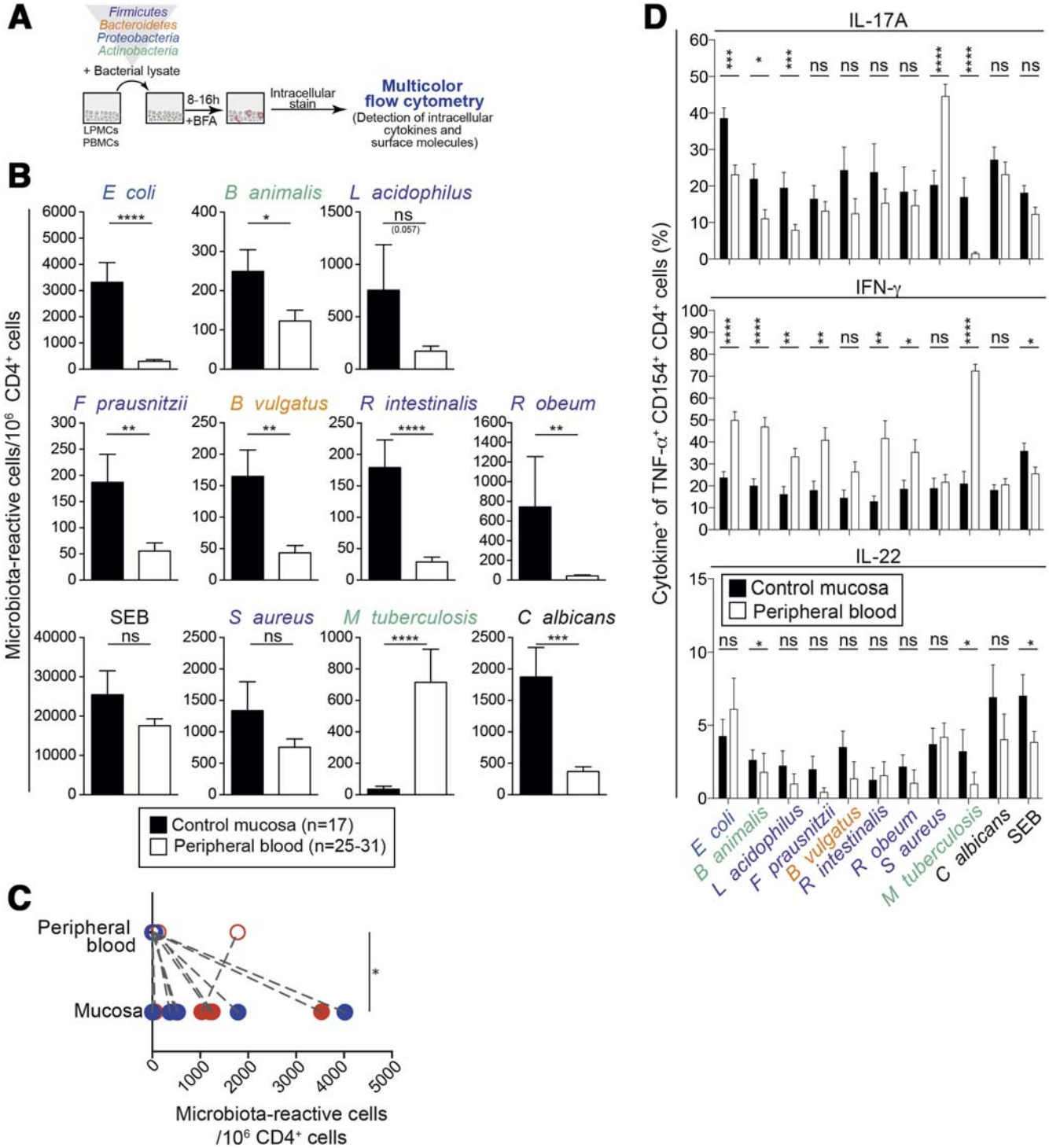


**Figure 3.** Microbiota-reactive CD4$^+$ T cells are enriched in gut tissue. Lamina propria mononuclear cells (LPMCs) were isolated from non-inflamed and tumor-free surgical specimens from colorectal cancer patients. (*A*) Experimental setup. LPMCs were stimulated with heat-inactivated bacteria for 8−12 hours and assessed for intracellular expression of cytokines and CD154. (*B*) Estimated microbiota-reactive cells per million CD4$^+$ T cells in adult blood and intestinal tissue from unrelated donors, based on CD154 staining (n = 17 for control mucosa; n = 25−31 for blood). (*C*) Matched LPMCs and PBMCs were stimulated with heat-inactivated *E coli* (*blue symbols*) or *S typhimurium* (*red symbols*), analyzed for CD154 expression, and compared with respect to the estimated microbiota-reactive cells per million CD4$^+$ T cells. *Connected dots* represent matched samples. (*D*) Frequencies (±SEM) of IL17A, IFN-gamma, and IL22 production by CD154$^+$TNF-$\alpha^+$ memory CD4$^+$ T cells isolated from LPMCs or PBMCs from unrelated donors after stimulation with heat-inactivated bacteria (n = 10−23 donors). Significance calculated between the respective stimulations in control mucosa and peripheral blood. Statistics: (*B*, *D*) Mann-Whitney test; (*C*) paired *t* test.

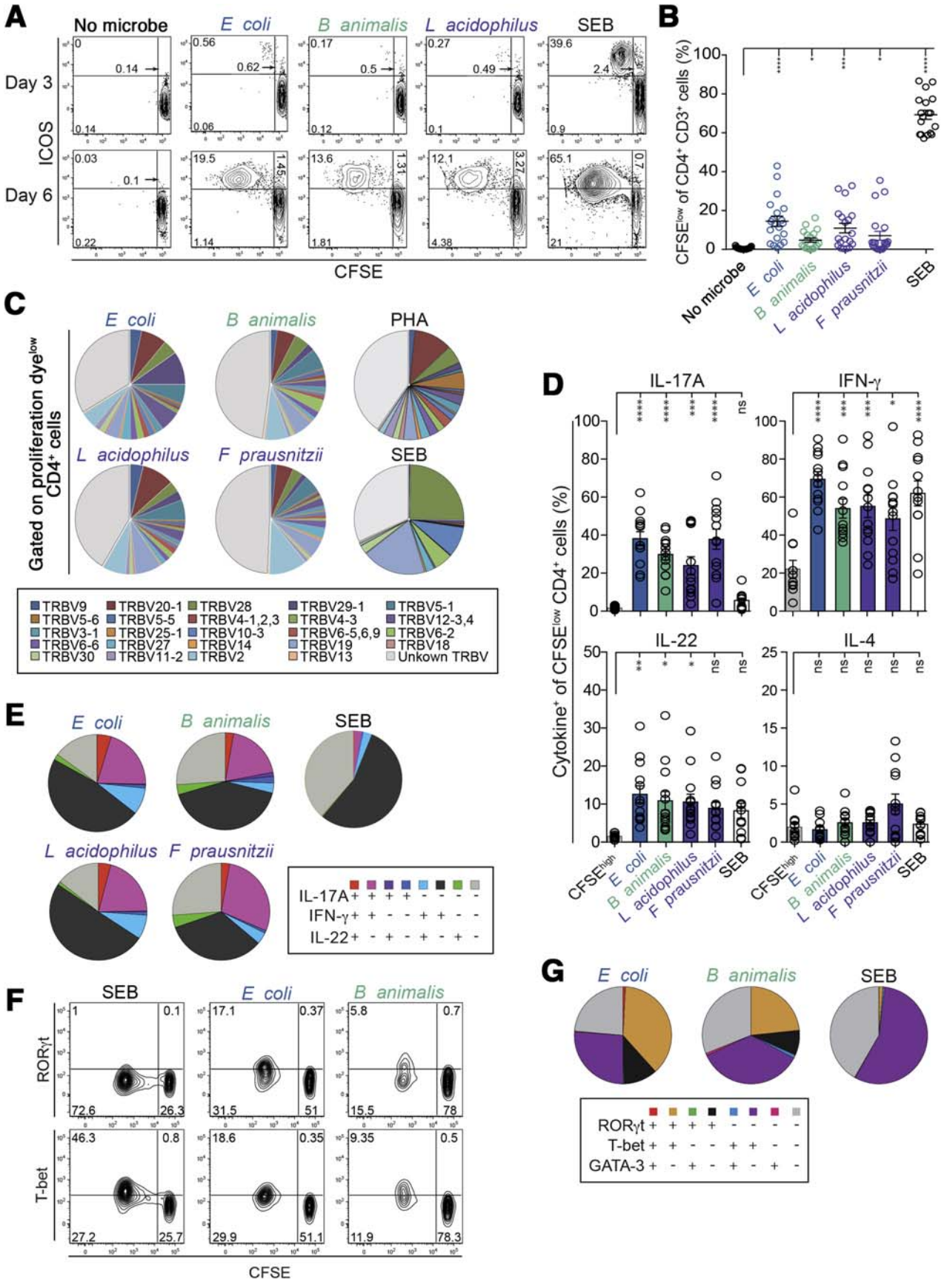
A
No microbe
E coli
B animalis
L acidophilus
SEB
Day 3
Day 6
ICOS
CFSE
B
CFSE^low of CD4^+ CD3^+ cells (%)
No microbe
E coli
B animalis
L acidophilus
F prausnitzii
SEB
C
E coli
B animalis
PHA
L acidophilus
F prausnitzii
SEB
Gated on proliferation dye^low CD4^+ cells
TRBV9
TRBV20-1
TRBV28
TRBV29-1
TRBV5-1
TRBV5-6
TRBV5-5
TRBV4-1,2,3
TRBV4-3
TRBV12-3,4
TRBV3-1
TRBV25-1
TRBV10-3
TRBV6-5,6,9
TRBV6-2
TRBV6-6
TRBV27
TRBV14
TRBV19
TRBV18
TRBV30
TRBV11-2
TRBV2
TRBV13
Unkown TRBV
D
IL-17A
IFN-γ
IL-22
IL-4
Cytokine^+ of CFSE^low CD4^+ cells (%)
CFSE^high
E coli
B animalis
L acidophilus
F prausnitzii
SEB
E
E coli
B animalis
SEB
L acidophilus
F prausnitzii
IL-17A
IFN-γ
IL-22
F
SEB
E coli
B animalis
RORγt
T-bet
CFSE
G
E coli
B animalis
SEB
RORγt
T-bet
GATA-3

flow cytometry after stimulation with enteric bacteria for 6 days. Enteric microbiota-reactive cells produced Th1- and Th17-related cytokines, including IFN-gamma, IL17A, and IL22, but only low amounts of the Th2 cytokine IL4, comparable to cells reactive toward *S aureus* or *C albicans* (Figure 4*D* and Supplementary Figure 5*B* and *C*). In contrast, memory T cells reactive toward SEB, *M tuberculosis*, influenza vaccine components, or tetanus toxoid showed a polarized Th1 profile with low expression of IL17A (Figure 4*D* and Supplementary Figure 5*B* and *C*). Boolean gating revealed a high degree of functional heterogeneity in expanded microbiota-reactive memory T cells, with frequent co-expression of IL17A, IL22, and IFN-gamma (Figure 4*E*). Bacteria-reactive cells co-expressed the transcription factors RAR-related orphan receptor γt and T-box expressed in T cells, which are characteristic of Th17 and Th1 cells, respectively (Figure 4*F* and *G* and Supplementary Figure 5*D* and *E*). Intriguingly, a subset of $CD4^+$ T cells reactive to *F prausnitzii*, *L acidophilus*, or *B animalis* produced the immunoregulatory cytokine IL10 in addition to IFN-gamma and IL17A (Supplementary Figure 5*F*). Compared to T cells that are reactive toward *M tuberculosis* or vaccine antigens, enteric microbiota-reactive T cells are functionally distinct and produce barrier-promoting and immunoregulatory cytokines.

## Microbiota-Reactive Memory T Cells Promote Intestinal Stromal and Epithelial Cell Activation

During periods of epithelial damage and exposure to commensals, activation of microbiota-reactive memory T cells could promote protective immune responses. To assess their tissue-modulating capabilities, cell-free supernatants of microbiota-reactive memory T cells were used to stimulate CCD18Co intestinal myofibroblasts and LIM1863 colonic epithelial cells. CCD18Co and LIM1863 cells were then assessed for expression of various immune response genes that were selected a priori to represent responses to major T-cell–derived cytokines. Both cell types responded by expressing several cytokine and chemokine genes known to be induced by IL17A (including *IL1B*, *CSF2*, *IL6*, *CXCL1*, and *CXCL8*), as well as IFN-gamma–inducible genes, including *CXCL9*, *CXCL10*, and *CXCL11* (Figure 5*A* and *B*).[31] Conversely, supernatants from SEB-stimulated memory T cells (which produce little IL17A) mainly induced IFN-gamma–dependent genes. Thus, stimulation of non-hematopoietic intestinal cells by microbiota-reactive T cells may promote recruitment and activation of myeloid cell populations to facilitate pathogen control and tissue repair.

We next assessed the effects of individual cytokines in *E coli*–reactive T-cell supernatants using combinations of neutralizing antibodies. This experiment revealed distinct IFN-gamma– and IL17A-/TNF-α–dependent groups of response genes in both intestinal epithelial cells and fibroblasts. IFN-gamma blockade strongly reduced expression of several chemokine genes, including *CXCL9*, *CXCL10*, *CXCL11*, *CCL2*, and *CCL7* (IFN-gamma–dependent module; Figure 5*C* and *D*). Intriguingly, single blockade of IL17A, IL22, or TNF-α did not affect stromal or epithelial cell activation (Figure 5*C* and *D*). However, combined blockade of IL17A and TNF-α influenced a large number of genes, including *CSF2*, *IL1B*, *TNF*, *CXCL1*, *CXCL8*, *CXCL5*, *CXCL6*, and *CCL20* (IL17A/TNF-α–dependent module). Triple blockade of IFN-gamma, IL17A, and TNF-α completely inhibited stromal and epithelial cell activation. IL22 blockade did not affect cytokine or chemokine production, but attenuated induction of the antimicrobial peptide *REG3G* in LIM1863 cells. Given that the products of T-cell–stimulated stromal and epithelial cells are highly expressed in the inflamed mucosa of IBD patients (Figures 5*E* and 7*D*), this signature might reflect the activation of microbiota-reactive T cells after epithelial disruption, a key feature of IBD.

## Microbiota-Reactive $CD4^+$ T Cells in Inflamed Intestinal Tissue Show a T-Helper 17–Skewed Phenotype in Patients With Inflammatory Bowel Disease

IBD is thought to arise in part from aberrant adaptive immune responses to microbiota.[8] Human $CD4^+$ T cells in IBD have been functionally characterized mainly by polyclonal stimulation.[32–34] Therefore, we evaluated microbiota-reactive $CD4^+$ T-cell responses in IBD patients using the CD154 detection approach. Circulating microbiota-reactive $CD4^+$ T-cell frequencies were decreased in IBD patients compared with healthy donors,



**Figure 4.** Microbiota-reactive memory $CD4^+$ T cells are clonally diverse and functionally heterogeneous. Memory $CD4^+$ T cells were labeled with CFSE or violet proliferation dye (VPD)-450 and stimulated with heat-inactivated bacteria in the presence of autologous monocytes. (*A*) CFSE profiles and inducible T-cell costimulator (ICOS) expression on days 3 and 6 of stimulation in a representative donor. (*B*) Percentage of $CFSE^{low}$ $CD4^+$ T cells of each individual donor (n = 18). (*C*) Pie charts showing TCR Vβ expression by proliferating $VPD^{low}$ cells measured by Vβ antibody staining on day 7 of stimulation. Average of 3 independent donors is depicted. TCR Vβ usage of the different reactivities of 3 independent donors is summarized in Supplementary Table 2. (*D*) Mean (±SEM) cytokine production frequencies of proliferating $CFSE^{low}$ cells and non-activated $CFSE^{high}$ cells after phorbol myristate acetate/ionomycin stimulation (n = 12–13 independent donors). (*E*) Boolean gating analysis showing each possible combination of IL17A, IFN-gamma, and IL22 production by $CFSE^{low}$ proliferating cells. Data from 9 independent donors. (*F*, *G*) RAR-related orphan receptor γt (RORγt) and T-box expressed in T cells (T-bet) expression in proliferating $CFSE^{low}$ cells measured by intracellular staining on day 7 of stimulation. (*G*) Boolean gating analysis showing each possible combination of RORγt, T-bet, and GATA-binding factor-3 production by $CFSE^{low}$ proliferating cells. Data from 3 independent donors. Statistics: (*B*) 1-way analysis of variance with Sidak's multiple comparison test; (*D*) 1-way analysis of variance with Bonferroni's multiple comparison test.

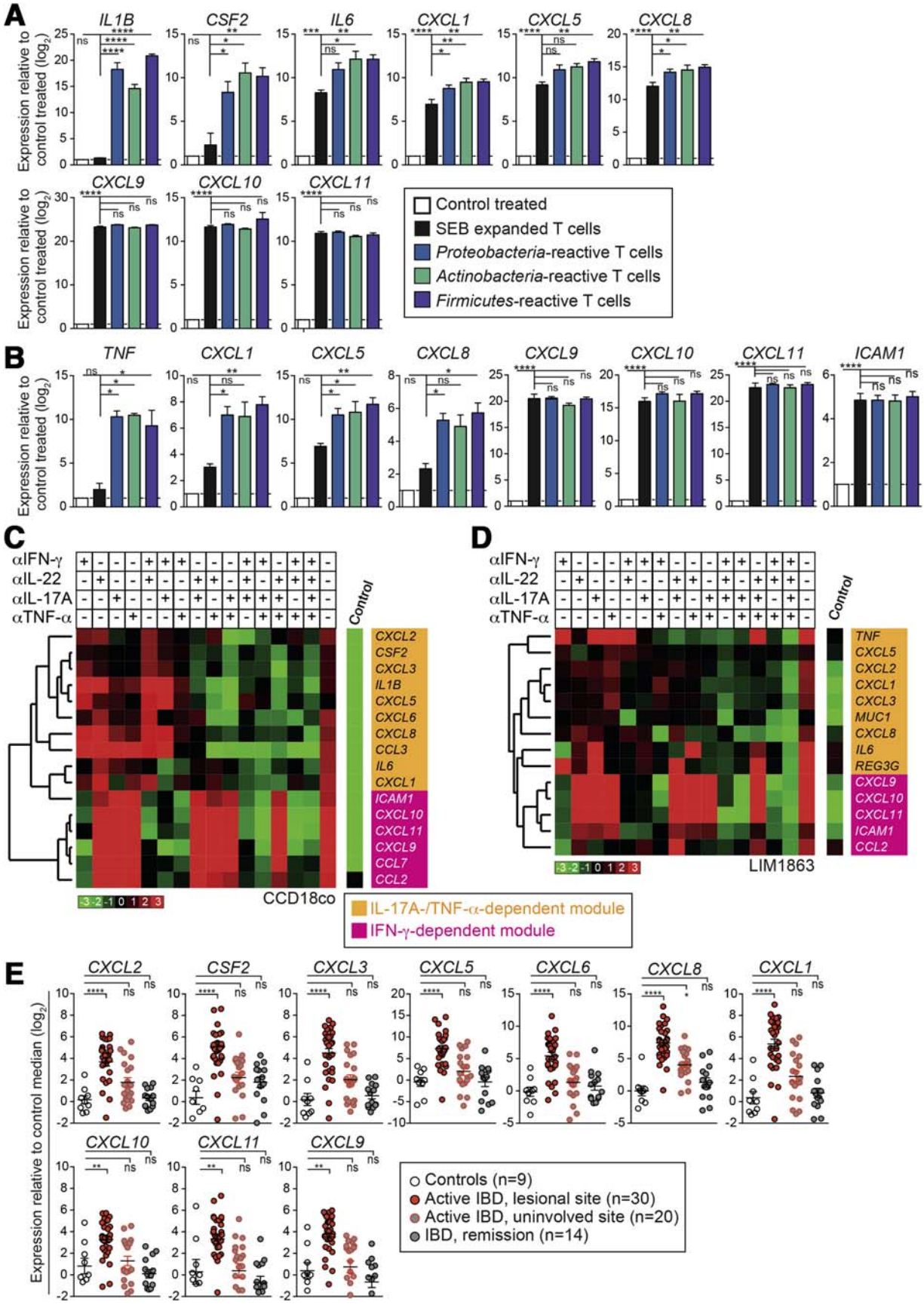
A
IL1B
CSF2
IL6
CXCL1
CXCL5
CXCL8
CXCL9
CXCL10
CXCL11
Expression relative to control treated (log2)
Control treated
SEB expanded T cells
Proteobacteria-reactive T cells
Actinobacteria-reactive T cells
Firmicutes-reactive T cells
B
TNF
CXCL1
CXCL5
CXCL8
CXCL9
CXCL10
CXCL11
ICAM1
C
αIFN-γ
αIL-22
αIL-17A
αTNF-α
Control
CXCL2
CSF2
CXCL3
IL1B
CXCL5
CXCL6
CXCL8
CCL3
IL6
CXCL1
ICAM1
CXCL10
CXCL11
CXCL9
CCL7
CCL2
CCD18co
D
TNF
CXCL5
CXCL2
CXCL1
CXCL3
MUC1
CXCL8
IL6
REG3G
CXCL9
CXCL10
CXCL11
ICAM1
CCL2
LIM1863
IL-17A-/TNF-α-dependent module
IFN-γ-dependent module
E
CXCL2
CSF2
CXCL3
CXCL5
CXCL6
CXCL8
CXCL1
CXCL10
CXCL11
CXCL9
Expression relative to control median (log2)
Controls (n=9)
Active IBD, lesional site (n=30)
Active IBD, uninvolved site (n=20)
IBD, remission (n=14)

which might reflect their selective recruitment to the inflamed gut (Figure 6*A* and Supplementary Figure 6*A*). However, intestinal memory CD4$^+$ T cells from IBD patients did not display reciprocally higher frequencies of microbial specificity (Figure 6*B* and Supplementary Figure 6*B*). We next calculated the frequency of memory CD4$^+$ T cells in inflamed mucosae using flow cytometry. Memory CD4$^+$ T cells were present at higher frequencies in inflamed tissue from IBD patients compared with tissue from matched non-lesional sites of IBD patients and healthy controls (Figure 6*C*). These findings were confirmed using a previously published bioinformatics approach known as CIBERSORT in an independent cohort[35] (Supplementary Figure 6*C*). Based on both approaches, memory CD4$^+$ T cells are typically 2- to 4-fold more frequent in inflamed tissue from IBD patients compared with tissue from healthy controls. Because inflamed tissue contains a higher abundance of memory CD4$^+$ T cells than healthy mucosa, it can be inferred that gut-resident microbiota-reactive CD4$^+$ T cells are similarly enriched in patients with active IBD (Figure 6*C*, Supplementary Figure 6*C*).

To evaluate functional alterations in microbiota-reactive CD4$^+$ T cells in IBD, intracellular CD154 detection was combined with cytokine analysis. Compared with healthy controls, circulating microbiota-reactive CD4$^+$ T cells from IBD patients displayed increased IL17A and IL2 production, but decreased expression of IFN-gamma (Figure 7*A* and Supplementary Figure 6*D* and *E*). Interestingly, increased IL17A production was observed in all enteric bacteria-reactive responses, but not in *S aureus, M tuberculosis*, or SEB responses (Figure 7*A* and Supplementary Figure 6*E* and *F*). These changes were observed in both Crohn's disease and ulcerative colitis and were independent of disease activity or therapy (Supplementary Figure 6*G*). However, no difference in IL10 production was observed between healthy donors and IBD patients (Supplementary Figure 6*H*). IFN-gamma and IL17A co-expression is thought to identify pathogenic CD4$^+$ T cells in mouse colitis models,[36] so we assessed their co-expression in *E coli*–reactive memory CD4$^+$ T cells. Compared with controls, IBD patients displayed significantly increased frequencies of IL-17A$^+$IFN-gamma$^-$ cells and a marginal increase in IL17A$^+$IFN-gamma$^+$ cells, while the IL17A$^-$IFN-gamma$^+$ fraction was reduced significantly (Figure 7*B*). *E coli*–reactive CD4$^+$ T cells from inflamed intestinal tissue showed an increase in IL17A single producers similar to that seen in peripheral blood (Figure 7*C*).

Because the Th17-inducing cytokines *IL1B*, *IL6*, and *IL23A* were highly enriched in the inflamed intestinal tissue of IBD patients (Figure 7*D*), we reasoned that they might promote Th17 polarization of bacteria-reactive T cells. Indeed, treatment of microbiota-reactive CD4$^+$ T cells from healthy donors and IBD patients with IL1$\beta$, IL6, or IL23 for 1 week during stimulation with *E coli, S typhimurium, L acidophilus*, or *B animalis* (CFSE dilution assay) resulted in a 1.5- to 2-fold increase in IL17A production (Figure 7*E* and Supplementary Figure 6*I*).

Taken together, these experiments demonstrate that circulating and gut-resident microbiota-reactive CD4$^+$ T cells express increased frequencies of IL17A in IBD. Intestinal tissues from patients with active IBD express gene modules driven by Th1/Th17-derived cytokines, suggesting that bacteria-reactive memory cells could contribute to the tissue response.

## Discussion

The gastrointestinal tract harbors a large and diverse population of commensal bacteria, and how the immune system interacts with them is subject to intense investigation. Here we used 2 different methodologies to characterize microbiota-reactive CD4$^+$ T-cell frequencies and phenotypes in the blood and intestinal tissue of healthy individuals and those with IBD. For each bacterial strain tested, the healthy CD4$^+$ T-cell repertoire contains reactive cells at a frequency of 40–4000 per million, consistent with other antigen-reactive memory T cells.[37] Microbiota-reactive CD4$^+$ T cells were mainly of a memory phenotype, present in both blood and gut tissue, had a diverse TCR V$\beta$ repertoire, and showed little clonotype sharing. Notably, microbiota-reactive CD4$^+$ T cells were functionally heterogeneous in terms of homing receptor expression and



**Figure 5.** Microbiota-reactive memory T cells promote intestinal stromal and epithelial cell activation. Healthy donor memory CD4$^+$ T cells from peripheral blood were labeled with CFSE and stimulated with heat-inactivated bacteria in the presence of autologous monocytes. CD4$^+$CFSE$^{low}$ICOS$^{high}$cells were fluorescence-activated cell–sorted on day 7 and expanded for 10–14 days with anti-CD3/CD28 beads. Expanded cells were stimulated at equal numbers with phorbol myristate acetate (PMA)/ionomycin for 24 hours to produce conditioned supernatants. (*A*, *B*) Cell-free supernatants from different T-cell specificities were used to stimulate CCD18Co intestinal myofibroblasts and LIM1863 colon epithelial cells. Gene expression in stimulated cells was measured by quantitative polymerase chain reaction (qPCR) and normalized to control treatment (media containing PMA/ionomycin alone). Results of independent stimulations were pooled together into the following categories: *Proteobacteria*-reactive T cells (*S typhimurium*– and *E coli*–reactive); *Actinobacteria*-reactive T cells (*B animalis*-reactive); *Firmicutes*-reactive T cells (*F prausnitzii*– and *L acidophilus*–reactive). Data are from 3 independent T-cell donors. (*C*, *D*) Supernatants from *E coli*–reactive CD4$^+$ T cells were used to stimulate CCD18Co (*C*) or LIM1863 (*D*) cells. Supernatants were pretreated with 1 or more cytokine-neutralizing antibodies as indicated. Gene expression was median-normalized, $\log_2$ transformed, and plotted as a heat map. Data representative of 2–3 independent experiments. (*E*) qPCR analysis of mucosal biopsies from the Oxford IBD cohort, categorized by endoscopic assessment of disease activity. Demographic and clinical characteristics of IBD patients are summarized in Supplementary Table 5. Statistics: (*A*, *B*, *E*) 1-way analysis of variance with Sidak's multiple comparison test.

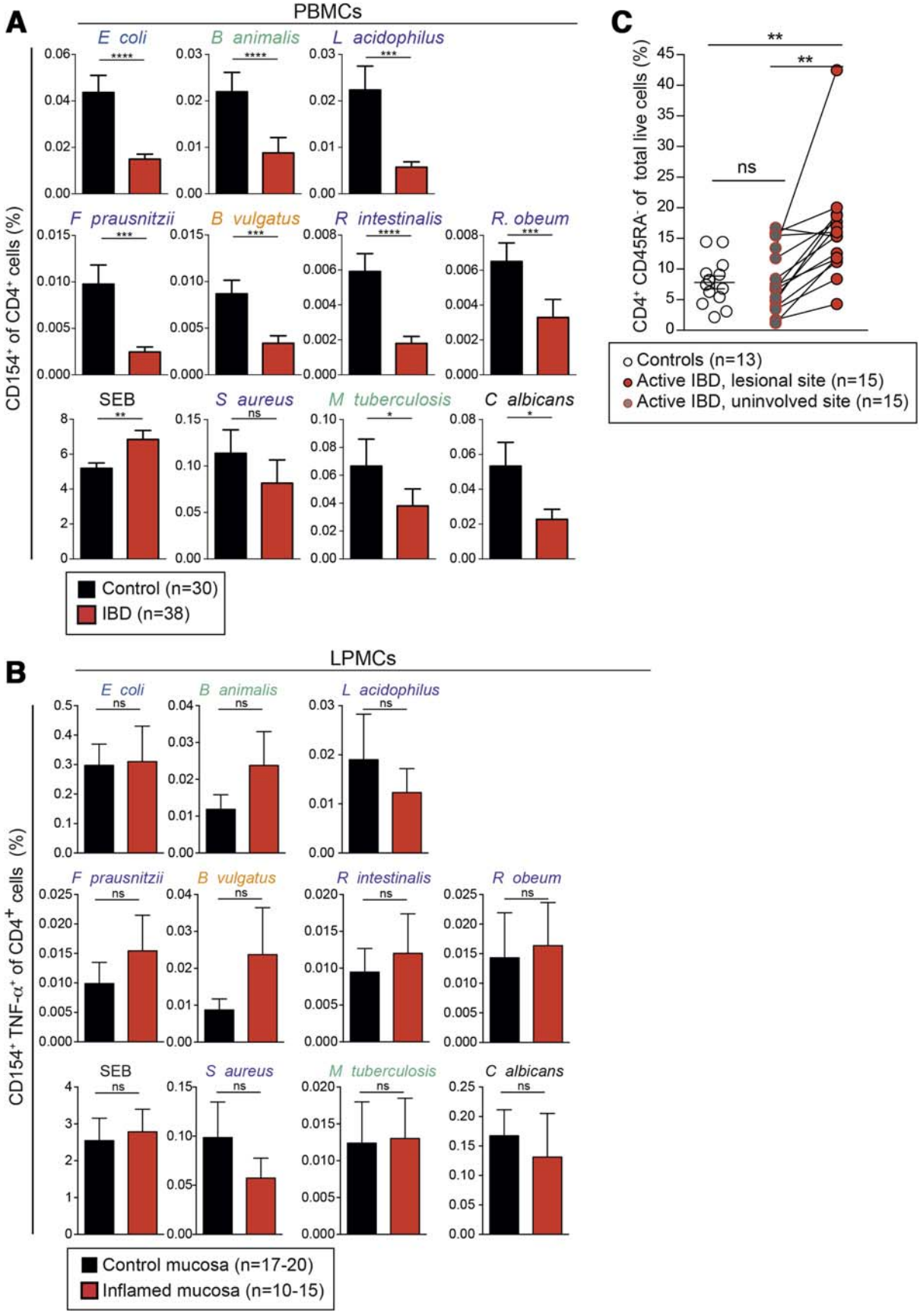
A
PBMCs
E coli
B animalis
L acidophilus
F prausnitzii
B vulgatus
R intestinalis
R. obeum
SEB
S aureus
M tuberculosis
C albicans
CD154+ of CD4+ cells (%)
Control (n=30)
IBD (n=38)
B
LPMCs
CD154+ TNF-α+ of CD4+ cells (%)
Control mucosa (n=17-20)
Inflamed mucosa (n=10-15)
C
CD4+ CD45RA- of total live cells (%)
ns
Controls (n=13)
Active IBD, lesional site (n=15)
Active IBD, uninvolved site (n=15)

effector functions and could stimulate intestinal cells via production of IL17*A*, IFN-gamma, IL22, and TNF-$\alpha$. In addition, microbiota-reactive $CD4^+$ T cells were recruited to sites of inflammation and showed increased IL17A production in patients with IBD.

Characterizing T-cell responses to bacteria is technically challenging due to their complex antigenic makeup. We therefore used the CD154 and CFSE dilution assays, both of which exploit microbial complexity, to provide large numbers of antigens. The combination of CFSE dilution and TCR V$\beta$ sequencing allowed us to quantify clonotype heterogeneity and sharing between different bacteria-reactive T cells. Given the phylogenetic similarity of several bacteria used in this study, the paucity of clonotype sharing was surprising. Nevertheless, enteric bacteria-reactive T cells could be cross-reactive to other antigens not assessed in this study, and may have been primed during immune responses to other targets.[38] High interclonal and intraclonal functional heterogeneity in human $CD4^+$ T-cell responses to microbes and vaccines was observed recently.[19] However, clonotype sharing between different microbial stimuli has not been studied previously and requires further investigation.

Microbiota-reactive $CD4^+$ T cells showed substantial phenotypic and functional heterogeneity. The majority of circulating enteric bacteria-reactive $CD4^+$ T cells co-expressed chemokine receptors, including CCR4, CCR6, and CCR7, while a smaller fraction expressed the gut-related homing receptors $\alpha4\beta7$ and CCR9. These receptors promote access to secondary lymphoid organs and various mucosal tissues, including the intestine.[4,27] In addition, circulating and gut-resident microbiota-reactive T cells displayed both Th17 and Th1 characteristics and, in some cases, produced IL10.[39] Gut-resident cells showed a clear Th17 bias when compared to circulating populations, which was more pronounced in IBD.

Based on our observations, we can speculate that continuous sampling of luminal antigens by intestinal dendritic cells causes low-level stimulation of gut-resident $CD4^+$ T cells to produce cytokines that support epithelial integrity, barrier function, and intestinal homeostasis.[40,41] Indeed, cytokine production by commensal-reactive $CD4^+$ T cells might play a more significant role in supporting gut homeostasis than previously thought (Supplementary Figure 7). However, this homeostatic circuit might be disrupted in IBD due to dysbiotic changes and/or perturbed myeloid cell activity, causing inappropriate T-cell activation and a pathogenic imbalance of cytokine production.[8]

While IL17A is frequently cited as a pathogenic cytokine, it is also critical for promoting mucosal barrier function and protection from pathogens.[31] Absence of IL17A was recently shown to increase epithelial injury and compromise barrier function in mouse models of colitis.[42,43] Indeed, IL17A is a critical driver of neutrophil recruitment, and its absence could therefore exacerbate mucosal inflammation by facilitating bacterial invasion and dispersal.[44] Notably, blockade of IL17A in Crohn's disease caused disease exacerbation, despite being well tolerated and therapeutically effective in psoriasis.[45] Thus, IL17A likely plays a key tissue-protective role in humans, suggesting that the increased Th17 polarization of microbiota-reactive T cells in IBD patients could reflect an effort to bolster tissue integrity.

Host-microbial homeostasis depends on minimizing contact between micro-organisms and mucosal surfaces via the combined action of epithelial cells, mucus, IgA, antimicrobial peptides, and immune cells.[1,2] Active immune responses to gut flora have been linked to disease.[8] However, this concept should be revisited in light of our current findings and the observation that healthy individuals generate antibody responses to commensals.[46,47] At least 2 plausible mechanisms could explain the genesis of these microbiota-reactive responses. First, mucosal dendritic cells constantly survey the luminal microenvironment and thereafter migrate to secondary lymphoid tissues to initiate B- and T-cell responses.[48,49] Second, during gastrointestinal infections in mice, immune responses against commensals and pathogens are induced in parallel.[50] Continuous luminal sampling of intestinal microbiota and periodic epithelial breaches during gastrointestinal infections might provide a plethora of memory T cells with potential reactivity toward newly encountered pathogens.[6,7] Therefore, contrary to the notion that they promote inflammatory pathology, acquired commensal-reactive T-cell responses may be essential to promote barrier function and IL10-mediated immune regulation—2 cornerstones of intestinal homeostasis.



**Figure 6.** Abundance of circulating and gut-resident enteric bacteria-reactive $CD4^+$ T cells in IBD. (*A*) PBMCs from healthy donors or IBD patients were stimulated with the indicated heat-inactivated bacteria and analyzed for CD154 expression. Frequencies (±SEM) of $CD154^+$ cells among $CD4^+$ T cells are depicted (n = 30–38). Demographic and clinical characteristics of IBD patients are summarized in Supplementary Table 6. (*B*) Lamina propria mononuclear cells (LPMCs) were isolated from inflamed surgical specimens from IBD patients or non-inflamed and tumor-free surgical specimens from colorectal cancer patients. Isolated LPMCs were stimulated with the indicated heat-inactivated bacteria and analyzed for CD154 expression. Frequencies (±SEM) of $CD154^+$ cells among $CD4^+$ T cells are depicted (n = 10–20). (*C*) LPMCs from endoscopic intestinal biopsies were obtained from healthy controls or matched lesional and non-lesional sites of IBD patients from an independent Oxford cohort (n = 12 controls and 17 IBD). *Dots* represent frequencies of $CD45RA^-CD4^+$ memory T cells among total live LPMCs from different donors; *connected dots* represent matched biopsies. Demographic and clinical characteristics of IBD patients are summarized in Supplementary Table 7. Statistics: (*A*, *B*, *C*) Mann-Whitney test; (*C*) 1-way analysis of variance with Sidak's multiple comparison test.

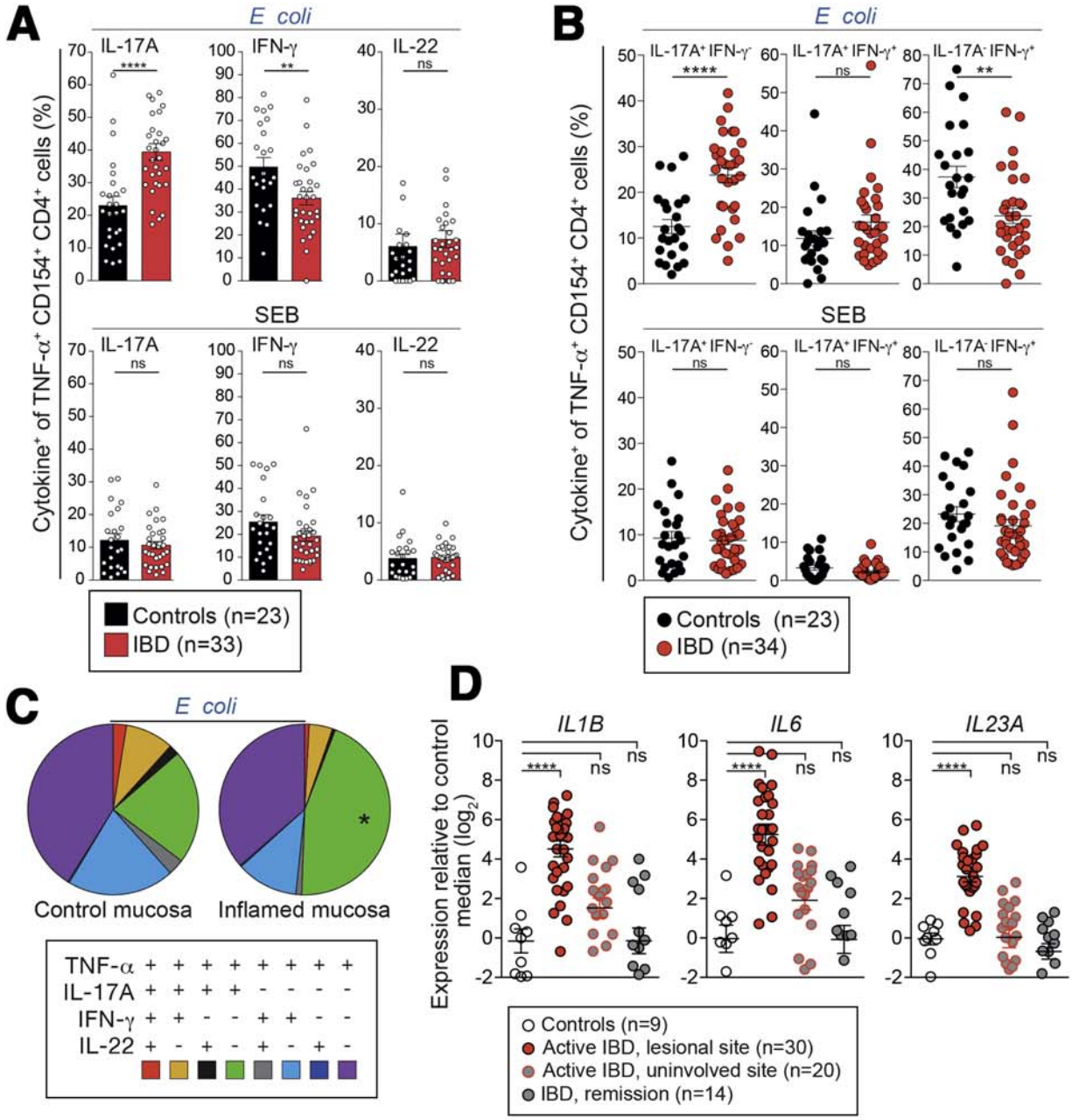
A
E coli
IL-17A
IFN-γ
IL-22
SEB
Cytokine+ of TNF-α+ CD154+ CD4+ cells (%)
Controls (n=23)
IBD (n=33)
B
E coli
IL-17A+ IFN-γ-
IL-17A+ IFN-γ+
IL-17A- IFN-γ+
SEB
Cytokine+ of TNF-α+ CD154+ CD4+ cells (%)
Controls (n=23)
IBD (n=34)
C
E coli
Control mucosa
Inflamed mucosa
TNF-α + + + + + + + +
IL-17A + + + + - - - -
IFN-γ + + - - + + - -
IL-22 + - + - + - + -
D
IL1B
IL6
IL23A
Expression relative to control median (log2)
Controls (n=9)
Active IBD, lesional site (n=30)
Active IBD, uninvolved site (n=20)
IBD, remission (n=14)
E
IL-17A
IFN-γ
Cytokine+ (relative to control)
IL-1β
IL-6
IL-23

## Supplementary Material

Note: To access the supplementary material accompanying this article, visit the online version of *Gastroenterology* at www.gastrojournal.org, and at https://doi.org/10.1053/j.gastro.2017.07.047.

## References


1. Littman DR, Pamer EG. Role of the commensal microbiota in normal and pathogenic host immune responses. Cell Host Microbe 2011;10:311–323.
2. Macpherson AJ, Slack E, Geuking MB, et al. The mucosal firewalls against commensal intestinal microbes. Semin Immunopathol 2009;31:145–149.
3. Honda K, Littman DR. The microbiome in infectious disease and inflammation. Annu Rev Immunol 2012;30:759–795.
4. Farber DL, Yudanin NA, Restifo NP. Human memory T cells: generation, compartmentalization and homeostasis. Nat Rev Immunol 2014;14:24–35.
5. Belkaid Y, Bouladoux N, Hand TW. Effector and memory T cell responses to commensal bacteria. Trends Immunol 2013;34:299–306.
6. Su LF, Kidd BA, Han A, et al. Virus-specific CD4(+) memory-phenotype T cells are abundant in unexposed adults. Immunity 2013;38:373–383.
7. Campion SL, Brodie TM, Fischer W, et al. Proteome-wide analysis of HIV-specific naive and memory CD4 +T cells in unexposed blood donors. J Exp Med 2014;211:1273–1280.
8. Maloy KJ, Powrie F. Intestinal homeostasis and its breakdown in inflammatory bowel disease. Nature 2011;474:298–306.
9. Cong Y, Brandwein SL, McCabe RP, et al. CD4+ T cells reactive to enteric bacterial antigens in spontaneously colitic C3H/HeJBir mice: increased T helper cell type 1 response and ability to transfer disease. J Exp Med 1998;187:855–864.
10. Duchmann R, Kaiser I, Hermann E, et al. Tolerance exists towards resident intestinal flora but is broken in active inflammatory bowel disease (IBD). Clin Exp Immunol 1995;102:448–455.
11. Duchmann R, May E, Heike M, et al. T cell specificity and cross reactivity towards enterobacteria, bacteroides, bifidobacterium, and antigens from resident intestinal flora in humans. Gut 1999;44:812–818.
12. Ergin A, Syrbe U, Scheer R, et al. Impaired peripheral Th1 CD4+ T cell response to Escherichia coli proteins in patients with Crohn's disease and ankylosing spondylitis. J Clin Immunol 2011;31:998–1009.
13. Chattopadhyay PK, Yu J, Roederer M. A live-cell assay to detect antigen-specific CD4+ T cells with diverse cytokine profiles. Nat Med 2005;11:1113–1117.
14. Frentsch M, Arbach O, Kirchhoff D, et al. Direct access to CD4+ T cells specific for defined antigens according to CD154 expression. Nat Med 2005;11:1118–1124.
15. Duncan SH, Louis P, Flint HJ. Cultivable bacterial diversity from the human colon. Lett Appl Microbiol 2007;44:343–350.
16. Kostic AD, Xavier RJ, Gevers D. The microbiome in inflammatory bowel disease: current status and the future ahead. Gastroenterology 2014;146:1489–1499.
17. Bosca-Watts MM, Tosca J, Anton R, et al. Pathogenesis of Crohn's disease: bug or no bug. World J Gastrointest Pathophysiol 2015;6:1–12.
18. Gradel KO, Nielsen HL, Schønheyder HC, et al. Increased short- and long-term risk of inflammatory bowel disease after salmonella or campylobacter gastroenteritis. Gastroenterology 2009;137:495–501.
19. Becattini S, Becattini S, Latorre D, et al. Functional heterogeneity of human memory CD4+ T cell clones primed by pathogens or vaccines. Science 2015;347:400–406.
20. Zielinski CE, Mele F, Aschenbrenner D, et al. Pathogen-induced human TH17 cells produce IFN-$\gamma$ or IL-10 and are regulated by IL-1$\beta$. Nature 2012;484:514–518.
21. Black GF, Weir RE, Chaguluka SD, et al. Gamma interferon responses induced by a panel of recombinant and purified mycobacterial antigens in healthy, non-mycobacterium bovis BCG-vaccinated Malawian young adults. Clin Vaccine Immunol 2003;10:602–611.
22. Lindestam Arlehamn CS, Paul S, Mele F, et al. Immunological consequences of intragenus conservation of


**Figure 7.** Microbiota-reactive $CD4^+$ T cells show a Th17-skewed phenotype in IBD patients. (*A, B*) PBMCs isolated from healthy donors and IBD patients were stimulated with heat-inactivated bacteria or SEB and analyzed for intracellular CD154 and cytokine expression. (*A*) Frequencies (±SEM) of IL17A, IFN-gamma, and IL22 expression in $CD154^+TNF\text{-}\alpha^+$ memory $CD4^+$ T cells (n = 23−33 independent donors). Demographic and clinical characteristics of IBD patients are summarized in Supplementary Table 6. (*B*) Frequencies (±SEM) of IL17A and IFN-gamma co-expression in $CD154^+TNF\text{-}\alpha^+$ memory $CD4^+$ T cells after short-term stimulation with heat-inactivated bacteria (n = 23−34 independent donors). (*C*) Lamina propria mononuclear cells (LPMCs) from inflamed IBD surgical specimens or non-inflamed and tumor-free surgical specimens from colorectal cancer patients were stimulated with heat-inactivated *E coli.* Boolean gating shows each possible combination of IL17A, IFN-gamma, and IL22 production by $CD154^+TNF\text{-}\alpha^+$ memory $CD4^+$ T cells (n = 6 and n = 7 independent donors for IBD and controls, respectively). (*D*) Quantitative polymerase chain reaction analysis of *IL1B, IL6*, and *IL23A* in intestinal mucosal specimens categorized by endoscopic assessment of disease activity. Demographic and clinical characteristics of IBD patients are summarized in Supplementary Table 5. (*E*) $CD4^+CD45RO^+CD45RA^-CD25^-CD8^-$ memory $CD4^+$ T cells were isolated from healthy donor blood, labeled with CFSE, and stimulated with autologous monocytes pulsed with *B animalis* in the presence or absence of the indicated cytokines. Data represent mean (±SEM) fold-changes in IL17A or IFN-gamma expression frequencies relative to cells expanded without cytokines. Statistics: (*A, B, C*) Mann-Whitney test; (*D, E*) 1-way analysis of variance with Sidak's multiple comparison test.

*Mycobacterium tuberculosis* T-cell epitopes. Proc Natl Acad Sci U S A 2015;112:E147–E155.
23. Matamoros S, Gras-Leguen C, Le Vacon F, et al. Development of intestinal microbiota in infants and its impact on health. Trends Microbiol 2013;21:167–173.
24. Appay V, van Lier RAW, Sallusto F, et al. Phenotype and function of human T lymphocyte subsets: consensus and issues. Cytometry A 2008;73:975–983.
25. Mascher B, Schlenke P, Seyfarth M. Expression and kinetics of cytokines determined by intracellular staining using flow cytometry. J Immunol Methods 1999; 223:115–121.
26. Moser B, Loetscher P. Lymphocyte traffic control by chemokines. Nat Immunol 2001;2:123–128.
27. Mueller SN, Gebhardt T, Carbone FR, et al. Memory T cell subsets, migration patterns, and tissue residence. Annu Rev Immunol 2013;31:137–161.
28. Keshav S, Wendt E. CCR9 antagonism: potential in the treatment of inflammatory bowel disease. Clin Exp Gastroenterol 2015;8:119–130.
29. Neurath MF. New targets for mucosal healing and therapy in inflammatory bowel diseases. Mucosal immunol 2014;7:6–19.
30. Kappler J, Kotzin B, Herron L, et al. V beta-specific stimulation of human T cells by staphylococcal toxins. Science 1989;244:811–813.
31. Ouyang W, Kolls JK, Zheng Y. The biological functions of T helper 17 cell effector cytokines in inflammation. Immunity 2008;28:454–467.
32. Annunziato F, Annunziato F, Cosmi L, et al. Phenotypic and functional features of human Th17 cells. J Exp Med 2007;204:1849–1861.
33. Kleinschek MA, Boniface K, Sadekova S, et al. Circulating and gut-resident human Th17 cells express CD161 and promote intestinal inflammation. J Exp Med 2009; 206:525–534.
34. Globig A-M, Hennecke N, Martin B, et al. Comprehensive intestinal T Helper cell profiling reveals specific accumulation of IFN-γ+IL-17+coproducing CD4+ T cells in active inflammatory bowel disease. Inflamm Bowel Dis 2014;20:2321–2329.
35. Newman AM, Liu CL, Green MR, et al. Robust enumeration of cell subsets from tissue expression profiles. Nat Methods 2015;12:453–457.
36. Shale M, Schiering C, Powrie F. CD4(+) T-cell subsets in intestinal inflammation. Immunol Rev 2013;252: 164–182.
37. Bacher P, Scheffold A. New technologies for monitoring human antigen-specific T cells and regulatory T cells by flow-cytometry. Curr Opin Pharmacol 2015;23:17–24.
38. Mason D. A very high level of crossreactivity is an essential feature of the T-cell receptor. Immunol Today 1998;19:395–404.
39. Sallusto F. Heterogeneity of human CD4 +T cells against microbes. Annu Rev Immunol 2016;34:317–334.
40. Blaschitz C, Raffatellu M. Th17 cytokines and the gut mucosal barrier. J Clin Immunol 2010;30:196–203.
41. Sonnenberg GF, Fouser LA, Artis D. Border patrol: regulation of immunity, inflammation and tissue homeostasis at barrier surfaces by IL-22. Nat Immunol 2011;12:383–390.
42. Maxwell JR, Zhang Y, Brown WA, et al. Differential roles for interleukin-23 and interleukin-17 in intestinal immunoregulation. Immunity 2015;43:739–750.
43. Lee JS, Tato CM, Joyce-Shaikh B, et al. Interleukin-23-independent IL-17 production regulates intestinal epithelial permeability. Immunity 2015;43:727–738.
44. Smith AM, Rahman FZ, Hayee B, et al. Disordered macrophage cytokine secretion underlies impaired acute inflammation and bacterial clearance in Crohn's disease. J Exp Med 2009;206:1883–1897.
45. Yang J, Sundrud MS, Skepner J, et al. Targeting Th17 cells in autoimmune diseases. Trends Pharmacol Sci 2014;35:493–500.
46. **Palm NW, de Zoete MR**, Cullen TW, et al. Immunoglobulin A coating identifies colitogenic bacteria in inflammatory bowel disease. Cell 2014;158:1000–1010.
47. Zeng MY, Cisalpino D, Varadarajan S, et al. Gut microbiota-induced immunoglobulin G controls systemic infection by symbiotic bacteria and pathogens. Immunity 2016;44:647–658.
48. Rescigno M, Urbano M, Valzasina B, et al. Dendritic cells express tight junction proteins and penetrate gut epithelial monolayers to sample bacteria. Nat Immunol 2001;2:361–367.
49. Macpherson AJ. Induction of protective IgA by intestinal dendritic cells carrying commensal bacteria. Science 2004;303:1662–1665.
50. Hand TW, Santos Dos LM, Bouladoux N, et al. Acute gastrointestinal infection induces long-lived microbiota-specific T cell responses. Science 2012;337: 1553–1556.



**Author names in bold designate shared co-first authorship.**

**Received July 7, 2016. Accepted July 25, 2017.**

**Reprint requests**
Address requests for reprints to: Fiona Powrie, FRS, Kennedy Institute of Rheumatology, University of Oxford, Roosevelt Drive, Headington, Oxford, OX3 7FY, United Kingdom. e-mail: Fiona.Powrie@kennedy.ox.ac.uk.

**Acknowledgments**
The authors thank Helen Ferry, Jenny Middleton, Sam Bullers, Sebastian Rogatti Granados, Priya Siddhanathi, James Chivenga, Ngonidzashe Charumbira, Jennifer Hollis, Linda Holden, Fiona Goddard, Karen Doig, Nicole Stoesser, Nicole Gordon, and Claire Pearson for fluorescence-activated cell sorting, technical support, patient sample collection, and laboratory management. The authors thank Harry Flint, Carolina V. Arancibia-Cárcamo, Emily Thornton, Tobias Schwerd, David Danko, Arnold Han, Mark Davis, M. Hussein Al-Mossawi, Paul Bowness, and all laboratory members for valuable support and discussions. The authors also thank Thomas Penz from the Biosequencing Facility at CeMM. The authors acknowledge the Oxford Radcliffe and GI Biobanks and the Oxford IBD cohort study supported by the National Institute for Health Research Oxford Biomedical Research Centre (grant no. HBRWAE04 Task HB81.G). The authors thank all volunteers and patients who took part in this study.

**Author contributions** ANH, NRW designed, performed, and analyzed experiments. ANH, NRW, and FP conceived and designed the project, interpreted data, and wrote the manuscript. MJTS analyzed TCR sequencing data. EW, KIMS, AD, ST, SC, BMJO, CD, SHD, and AB were involved in acquisition of data, data analysis, and interpretation of data. SAT, SK, HHU, AM provided essential materials and were involved in data interpretation and discussions. Oxford IBD Cohort Investigators provided IBD patient samples and ethical approval for the project.

Oxford IBD Cohort Investigators: Drs Carolina Arancibia, Adam Bailey, Ellie Barnes, Beth Bird-Lieberman, Oliver Brain, Barbara Braden, Jane Collier, James East, Lucy Howarth, Satish Keshav, Paul Klenerman, Simon Leedham, Rebecca Palmer, Fiona Powrie, Astor Rodrigues, Alison Simmons, Peter Sullivan, Simon Travis, and Holm Uhlig.

**Conflicts of interest**

These authors disclose the following: Fiona Powrie has received research support or consultancy fees from Eli Lilly, Merck, GSK, Janssen, Compugen, UCB, and MedImmune. Satish Keshav has received consulting fees and research support from ChemoCentryx Inc and GSK in the past. Holm H. Uhlig has project collaborations with Eli Lilly and UCB Pharma related to this project. Dr Keshav has provided consultancy services for a number of pharmaceutical and health care companies, including AbbVie, Actavis Allergan, Astra-Zeneca, Boehringer Ingelheim, ChemoCentryx, Dr Falk Pharma, Ferring, Gilead, GSK, Merck, Mitsubishi Tanabe Pharma, Pharmacosmos, Pfizer, Takeda, and Vifor Pharma, and has received research support from AbbVie, ChemoCentryx, GSK, and Merck. The remaining authors disclose no conflicts.

**Funding**

Ahmed N. Hegazy was supported by an EMBO long-term fellowship (ALTF 1161-2012) and a Marie Curie fellowship (PIEF-GA-2012-330621). Nathaniel R. West was supported by a Cancer Research Institute Irvington Postdoctoral Fellowship. Benjamin M. J. Owens was supported by an Oxford-UCB Pharma Postdoctoral Fellowship. Michael J. T. Stubbington and Sarah A. Teichmann were supported by European Research Council grant ThSWITCH and ThDEFINE (260507). Suzanne Campion and Andrew McMichael were supported by the Center for HIV/AIDS Vaccine Immunology and Immunogen Discovery (grant UM1-AI100645). The Rowett Institute of Nutrition and Health receives financial support from the Scottish Government Rural and Environmental Sciences and Analytical Services. Foundation Louis Jeantet, Wellcome Trust (Investigator award 095688/Z/11/Z), and European Research Council (ERC/HN/2013/21) supported Fiona Powrie and this project. Holm H. Uhlig is supported by the Crohn's & Colitis Foundation of America, and The Leona M. and Harry B. Helmsley Charitable Trust. Sylvia H. Duncan received financial support from the Scottish Government Rural and Environmental Sciences and Analytical Services.

# Supplementary Experimental Procedures

## Human Samples and Cell Isolation

PBMCs were isolated by Ficoll-Paque (GE Healthcare Life Sciences, Little Chalfont, UK) density gradient centrifugation, resuspended in phosphate-buffered saline with 2 mM EDTA and 0.02% bovine serum albumin, and further processed. Gut specimens were obtained from patients with IBD undergoing surgery for severe, chronically active, or complicated disease. Control gut specimens from macroscopically healthy areas were collected from colorectal cancer patients as non-inflammatory controls. One intestinal pinch biopsy was obtained from healthy donors (colorectal cancer screening, or other non-IBD related conditions) or IBD patients during routine endoscopy, from lesional, and non-lesional sites, attending the John Radcliffe Hospital (Oxford, UK). Inflammation status of biopsies was binarized into either inflamed or uninflamed categories based on endoscopic assessment. Additional information about the analyzed IBD patients can be found in Supplementary Tables 5−7.

Lamina propria mononuclear cells were isolated as described previously.[1] In brief, mucosa was dissected and washed in 1 mM dithiothreitol at room temperature for 15 minutes to remove mucus. Specimens were washed 3 times with 0.75 mM EDTA at 37°C for 45 minutes to detach epithelial crypts and digested overnight with 0.1 mg/mL collagenase D (Roche, Indianapolis, IN). Cells were centrifuged for 30 minutes in a Percoll gradient and collected at the 40%−60% interface. All solutions were supplemented with antibiotics (penicillin/streptomycin, 40 $\mu$g/mL gentamicin, and 0.025 $\mu$g/mL amphotericin B).

## Flow Cytometry

Cells were stained with the following monoclonal antibodies as described[2]: CD4-BV510 (OKT4), CD4 phycoerythrin (PE)-Dazzle (RPA-T4), CD3-PE-CF594 or –BV510 (UCHT1), CD45RA-BV711 (HI100), CD45RO-BV570 (UCHL1), CD161-eF450 (HP3G10), CCR7-PE (G034H7), CCR2-APC (K036C2), CCR6-BV605 (G034E3), CCR9-PE-Cy7 (L053E8), CXCR3-PE/Cy5 (1C6/CXCR3), CCR4-PE-Cy7 (1G1), CCR10-PE (314305), Integrin $\beta$7-FITC/APC (FIB504), CD69-PE-Cy7 (FN50), IL-2-BV650 (MQ1-17H12), TNF-$\alpha$-PB (MAb11), CD154-FITC/PE-Cy5 (24-31), IL-17A BV711 (eBio64DEC17), IL-22-PE-Cy7 (22URTI), IFN-$\gamma$-AF700 (B27), GM-CSF-APC (BVD2-21C11), and IL-4-PE (8D4-8) (eBioscience, Biolegend, San Diego, CA and Becton Dickinson, San Jose, CA). Fluorescein-activated cell sorting panels contained up to 12 fluorochromes. Compensation beads were used for compensations (BD Bioscience, San Jose, CA). TCR V$\beta$ usage was assessed using the IOTest Beta Mark TCR Vbeta Repertoire Kit (Beckman Coulter, Brea, CA). Samples were acquired on FACS LSRFortessa and FACSLSRII (Becton Dickinson); $\geq 2 \times 10^5$ memory $CD4^+$ T cells were acquired. Data were analyzed with FlowJo (Tree Star, Ashland, OR) and SPICE. For analysis of cytokine expression by microbiota-specific T cells, a minimum of 20 $CD4^+$ $CD154^+$ TNF-$\alpha^+$ T cells was used; donors with lower events were excluded.

## CD154 Enrichment of Antigen-Specific T Cells

For magnetic cell separation enrichment of $CD4^+CD154^+$ T cells, CD154 Enrichment and Detection Kit was used (Miltenyi Biotec). Briefly, cells were plated at $5 \times 10^6/cm^2$ for 7−12 hours with heat-inactivated bacteria in the presence of anti-CD40 blocking antibody (HB14) and anti-CD28 stimulation antibody (CD28.6). Anti-CD40 blockade prevents down-regulation of CD154, while CD28 co-stimulation optimizes induction of CD154 expression. For major histocompatibility complex II blockade, 10 $\mu$g/mL of a pan-HLA class-II blocking antibody (HLA-DR, DP, DQ; [Tü39]) was added 30 minutes before bacterial stimulation. Cord and adult blood analysis was performed identically. Antigen-presenting cell abundance is similar in cord and adult blood.[3,4]

## Cross-Reactivity Assay

$CD154^+$ $CD4^+$ T cells were isolated using magnetic cell separating enrichment and fluorescein activated cell sorting from total PBMCs after stimulation with *E coli Nissle* and *B animalis* lysates as described. $CD154^+$ $CD4^+$ T cells were expanded for 10−14 days with IL2 and anti-CD3/CD28 beads (beads/T cell ratio, 1:4, Dynals). The expanded T-cell lines were washed in IL2 free medium and incubated for 12 hours without IL2 in RPMI-1640 supplemented with 2 mM glutamine, 1% (v/v) non-essential amino acids, 1% (v/v) sodium pyruvate, penicillin (50 U/mL), streptomycin (50 mg/mL; all from Invitrogen), and 5% (v/v) human serum (National Blood Service, Bristol, UK). The expanded T-cell lines were labeled with CFSE, and then were co-incubated with autologous monocytes loaded with various bacterial lysates. T cells were co-cultured with the irradiated autologous monocytes at a ratio of 2:1 for 5−7 days. The CFSE dilution was measured at the end of the culture. Autologous $CD14^+$ monocytes were isolated from PBMC using anti-CD14 microbeads (Miltenyi Biotec) and frozen until the T-cell co-culture. Monocytes were thawed down, irradiated (45 Gy), and then pre-incubated for 3 hours with bacterial lysates before T-cell co-culture.

## Intracellular Cytokine Analysis

For intracellular cytokine staining, cells were restimulated with phorbol myristate acetate (5 ng/mL) and ionomycin (500 ng/mL; Sigma) or bacterial lysates. Brefeldin A (5 $\mu$g/mL; Sigma-Aldrich) was added at 2 hours. After 4−12 hours, cells were stained with fixable viability dye eFluor 780 (eBioscience) and surface markers, fixed with 2% formaldehyde (Merck), and stained for cytokines in buffer containing 0.05% saponin (Sigma-Aldrich). In some assays, cytokine analysis was combined with intracellular CD154 detection, as described previously.[5,6]

## Transcription Factors Staining

Transcription factor expression was analyzed using the FoxP3 staining buffer set (eBioscience) according to manufacturer's instructions. Briefly, cells were stained with fixable viability dye eFluor 780 (eBioscience) and surface

markers, fixed with 1× fixation/permeabilization buffer, followed by antibody staining and washing in 1× permeabilization buffer. T-box expressed in T cells−Pacific Blue (4B10) and GATA-binding factor-3−Alexa-647 (TWAJ) were from eBioscience. Related orphan receptor γt-PE (Q21-559) was from BD Bioscience.

### Preparation of Bacterial Lysates

Different bacteria were cultured in their respective optimal media for 16 hours at 37°C, washed in sterile phosphate-buffered saline and heat-inactivated at 65°C for 1 hour, followed by 3 freeze−thaw cycles. Extremely oxygen−sensitive bacteria were provided by Sylvia Duncan, University of Aberdeen, after heat inactivation. Suspensions were centrifuged at maximum speed for 15 minutes and supernatants collected. Protein concentration was quantified using Nanodrop (Thermo Fisher Scientific, Waltham, MA). The following bacterial strains were used: *B vulgatus* (Bv 1447), *B animalis* subsp *lactis* Bi-07, *C difficile* (OXF1003, Toxin AB$^-$), *E coli* (Nissle 1917), *F prauznitzii* (A2-165), *L acidophilus* (NCFM), *R intestinalis* (M50/1), *R obeum* (A2-162), *Salmonella enterica serovar typhimurium* (NCTC 12023), and *S aureus* (NCTC 6571). Additional information regarding the bacterial stains is provided in Supplementary Table 1. Bacterial lysates were titrated in CFSE dilution assay and an optimal concentration was used (5−15 μg/mL). Tetanus toxoid (Calbiochem, San Diego, CA) and influenza seasonal vaccine (OPTAFLU; Novartis, Basel, Switzerland) were used at 5 μg/mL. Heat-killed *M tuberculosis* (H37Ra) and *C albicans* were from InvivoGen (San Diego, CA). Ultrapure lipopolysaccharide-EB from *E coli* 0111:B4 (InvivoGen) was used as a stimulation control. SEB was used at 1 μEBmL (Sigma).

### RNA Extraction, Complementary DNA Synthesis, and Quantitative Polymerase Chain Reaction

Tissue was homogenized using a motor with sterile RNase/DNase-free disposable pestles (both VWR) in RLT buffer (Qiagen, Valencia, CA). Cells were lysed directly in RLT buffer. RNA was isolated using RNeasy Mini kit (Qiagen) or Quick-RNA MiniPrep kit (Zymo Research, Irvine, CA) followed by complementary DNA preparation using High-Capacity cDNA Reverse Transcription Kit (Applied Biosystems, Carlsbad, CA) with random hexamers. Quantitative polymerase chain reaction (PCR) was performed using a CFX96 (Bio-Rad, Hercules, CA) or ViiA7 384-well real-time PCR system (Applied Biosystems) with TaqMan assays (Life Technologies, Carlsbad, CA), and PrecisionPLUS Mastermix (Primerdesign, Southampton, UK). Expression levels were normalized to a housekeeping (hk) gene (*RPLP0*) and expressed as 2^-(CTgene-CThk). Heat maps were made using Cluster 3.0 and Java TreeView (Michael Eisen, Stanford University).

### CIBERSORT Analysis

To calculate enrichment of cell populations using CIBERSORT,[7] we analyzed the GSE16879 dataset on default settings. For each sample, relative expression of *PTPRC* (CD45, representing relative leukocyte content) was calculated separately using median-normalized microarray data. This value was then multiplied by CIBERSORT cell type scores (eg, proportion of memory CD4$^+$ T cells in the total leukocyte fraction) to estimate cell type enrichment levels. Finally, for cell types of interest, fold differences between IBD and control specimens were calculated to estimate relative cell type abundance in active IBD lesions versus healthy tissue.

### T-Cell Receptor Vβ Sequencing and Analysis

Memory T cells ($3.6 \times 10^6$) were cultured with autologous monocytes pulsed with heat-inactivated bacteria from 3 healthy donors. Expanded CFSE$^{low}$ ICOS$^+$CD4$^+$ T cells were sorted into DNase/RNase free water with bovine serum albumin (10 mg/mL) in 96-well plates (100 cells/well) and stored at −80°C. TCR Vβ sequence analysis was obtained by a series of 3 nested PCR reactions, as described previously.[8] Reverse transcription and preamplification were performed with a One-Step RT-PCR kit (Qiagen) using multiplex PCR with multiple Vβ region primers and a Cβ region primer. After the first reaction, an aliquot was used for the second PCR using a set of multiple internally nested TCR Vβ primers and internally nested Cβ region primer with HotStarTaq DNA polymerase kit (Qiagen). In the final PCR reaction, an aliquot of the second PCR was used and amplification was performed using barcoding primers containing the common 23-base sequence (incorporated into the second set of Vβ primers) and a third internally nested Cβ primer and Illumina Pair-End primers. After the third PCR reaction, each PCR product should have a unique set of barcodes incorporated that specifies plate, row, and column and have Illumina Paired-End sequences that enabled sequencing on the Illumina MiSeq platform. The PCR products were combined at equal proportion by volume, run on a 1.2% agarose gel, and a band around 350 to 380 bp was excised and gel purified using a Qiaquick gel extraction kit (Qiagen). Barcoded products were sequenced on the Illumina MiSeq platform.

Sequence reads were trimmed using 'Trim Galore' software (http://www.bioinformatics.babraham.ac.uk/projects/trim_galore/) with default settings. Reads were de-multiplexed using a custom Python script according to the presence of index sequences. A further custom script then split reads from each well according to the presence of primer sequences used in the PCR amplification. These reads were then analyzed by MICXR, version 1.6 (http://www.nature.com/nmeth/journal/v12/n5/full/nmeth.3364.html) using settings appropriate for the anticipated TCR locus of origin (A or B). MIXCR provided CDR3 sequences along with counts of the number of times each sequence was observed. Detected CDR3 sequences were filtered to exclude those with ≤10 counts per well. There were 48 wells per donor of SEB-stimulated or phytohemagglutinin-stimulated cells while there were 96 wells of bacterially stimulated cells. Furthermore, some wells did not contain any valid TCR sequences after filtering for low read counts, suggesting that amplification

or sequencing had failed for those wells. To permit comparisons of the number of TCR sequences between plates with differing numbers of successful wells, counts were scaled to the theoretical maximum of 96 wells.

## Supplementary References


1. Geremia A, Arancibia-Cárcamo CV, Fleming MPP, et al. IL-23-responsive innate lymphoid cells are increased in inflammatory bowel disease. J Exp Med 2011; 208:1127–1133.
2. Brodie T, Brenna E, Sallusto F. OMIP-018: chemokine receptor expression on human T helper cells. Cytometry A 2013;83:530–532.
3. Marodi L, Leijh PCJ, Furth RV. Characteristics and functional capacities of human cord blood granulocytes and monocytes. Pediatr Res 1984;18:1127–1131.
4. Sohlberg E, Saghafian-Hedengren S, Bremme K, et al. Cord blood monocyte subsets are similar to adult and show potent peptidoglycan-stimulated cytokine responses. Immunology 2011;133:41–50.
5. Frentsch M, Arbach O, Kirchhoff D, et al. Direct access to CD4+ T cells specific for defined antigens according to CD154 expression. Nat Med 2005;11:1118–1124.
6. Bacher P, Schink C, Teutschbein J, et al. Antigen-reactive T cell enrichment for direct, high-resolution analysis of the human naive and memory Th cell repertoire. J Immunol 2013;190:3967–3976.
7. Newman AM, Liu CL, Green MR, et al. Robust enumeration of cell subsets from tissue expression profiles. Nat Methods 2015;12:453–457.
8. Han A, Glanville J, Hansmann L, et al. Linking T-cell receptor sequence to functional phenotype at the single-cell level. Nat Biotechnol 2014;32:684–692.

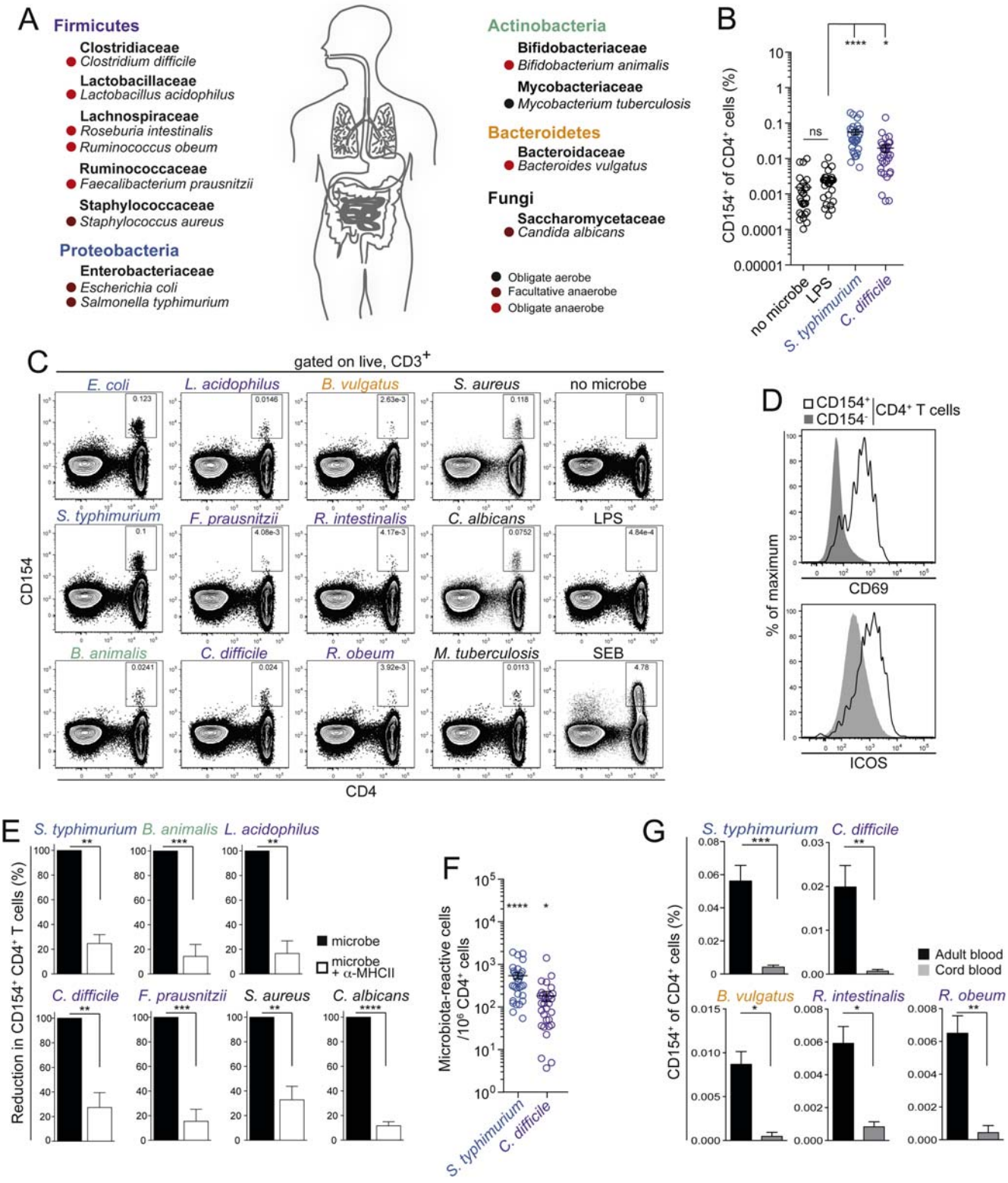
A
Firmicutes
Clostridiaceae
Clostridium difficile
Lactobacillaceae
Lactobacillus acidophilus
Lachnospiraceae
Roseburia intestinalis
Ruminococcus obeum
Ruminococcaceae
Faecalibacterium prausnitzii
Staphylococcaceae
Staphylococcus aureus
Proteobacteria
Enterobacteriaceae
Escherichia coli
Salmonella typhimurium
Actinobacteria
Bifidobacteriaceae
Bifidobacterium animalis
Mycobacteriaceae
Mycobacterium tuberculosis
Bacteroidetes
Bacteroidaceae
Bacteroides vulgatus
Fungi
Saccharomycetaceae
Candida albicans
Obligate aerobe
Facultative anaerobe
Obligate anaerobe
B
CD154+ of CD4+ cells (%)
ns
****
*
no microbe
LPS
S. typhimurium
C. difficile
C
gated on live, CD3+
E. coli
L. acidophilus
B. vulgatus
S. aureus
no microbe
S. typhimurium
F. prausnitzii
R. intestinalis
C. albicans
LPS
B. animalis
C. difficile
R. obeum
M. tuberculosis
SEB
CD154
CD4
D
CD154+
CD154-
CD4+ T cells
% of maximum
CD69
ICOS
E
S. typhimurium
B. animalis
L. acidophilus
C. difficile
F. prausnitzii
S. aureus
C. albicans
microbe
microbe + α-MHCII
Reduction in CD154+ CD4+ T cells (%)
F
Microbiota-reactive cells /10^6 CD4+ cells
S. typhimurium
C. difficile
G
S. typhimurium
C. difficile
B. vulgatus
R. intestinalis
R. obeum
Adult blood
Cord blood
CD154+ of CD4+ cells (%)

**Supplementary Figure 1.** Bacterial strains used in the study and detection of enteric bacteria-specific memory $CD4^+$ T cells (related to Figure 1). (*A*) Bacterial species are listed according to their family and phylum classification. *Colored circles* relate the bacteria to their gaseous requirement. (*B*) Frequencies of $CD154^+$ cells among peripheral $CD4^+$ T cells in adults after short-term stimulation with heat-inactivated bacteria. *Dots* represent different donors (n = 30). (*C*) Representative flow cytometric plots of different stimulations showing CD154 expression against CD4 within $CD3^+$ cells after short-term stimulation with heat-inactivated bacteria. Frequencies of CD154 within $CD4^+$ T cells are depicted. (*D*) Representative plot of CD69 and ICOS expression on $CD4^+CD154^+$ T cells after short-term stimulation with heat-inactivated *S typhimurium.* (*E*) PBMCs were stimulated with the indicated heat-inactivated bacteria in presence or absence of major histocompatibility complex II (MHCII) blocking antibodies and analyzed for CD154 expression. Percentage of reduction in $CD154^+$ frequencies after MHCII blockade compared to control treated is depicted. Frequencies (±SEM) of 3 independent experiments are depicted (n = 5–6 independent donors). (*F*) Estimated microbiota-reactive cells per million $CD4^+$ T cells in adult blood (n = 30). The numbers of microbiota-reactive T cells were calculated based on the frequencies of $CD4^+CD154^+$ T cells. Background (no microbe stimulation) was subtracted from bacterial stimulations. Significance calculated in relation to lipopolysaccharide (LPS) stimulation. (*G*) Frequencies ± SEM of $CD154^+$ cells among $CD4^+$ T cells in adult (n = 30) or cord blood (n = 3) after short-term stimulation with heat-inactivated bacteria. Statistics: (*E*, *G*) Mann-Whitney test; (*C*, *F*) 1-way analysis of variance with Sidak's multiple comparison test; ns, not significant; $^*P \leq .05$; $^{***}P \leq .01$; $^{***}P \leq .001$; $^{****}P \leq .0001$.

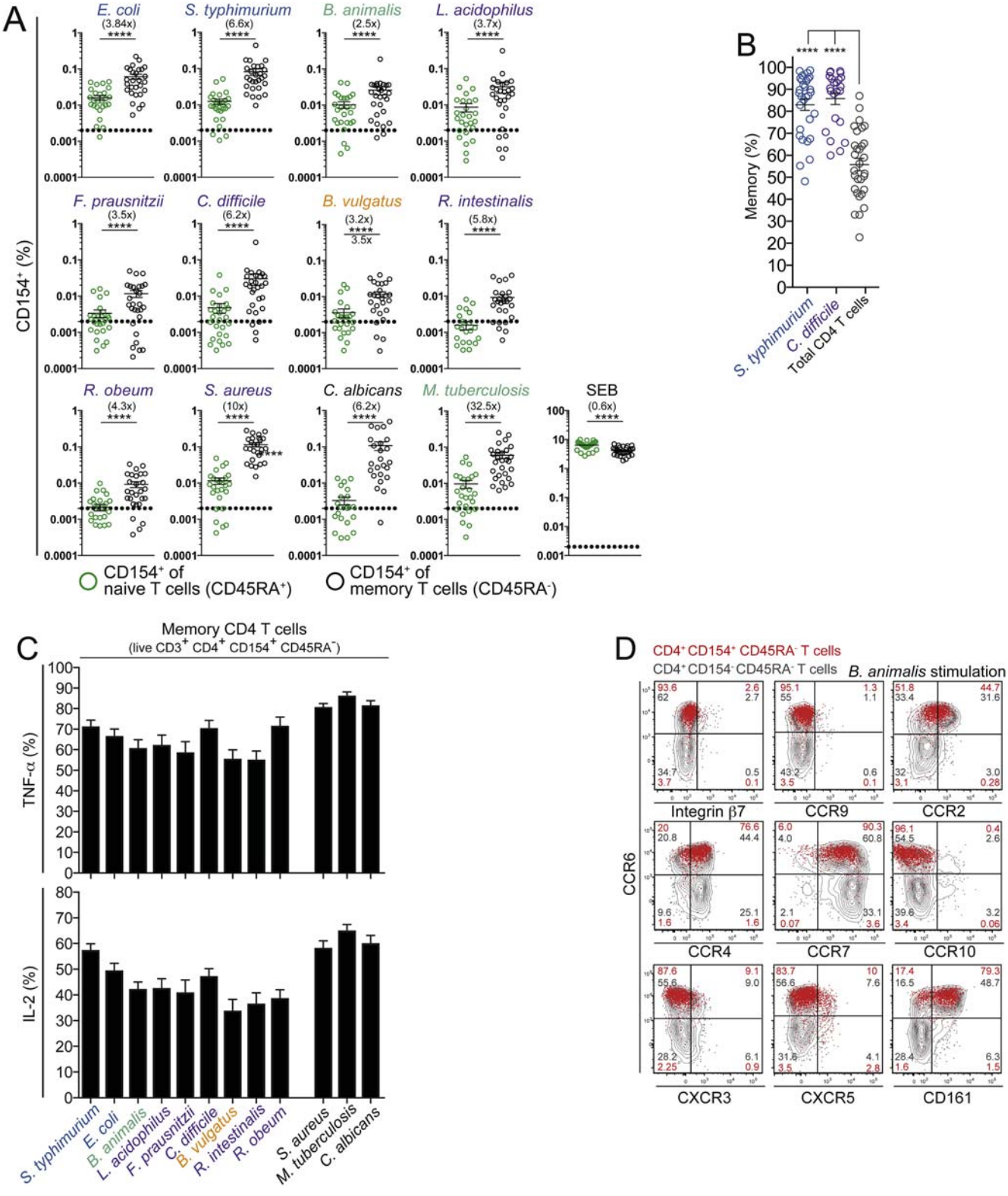
A
E. coli
(3.84x)
S. typhimurium
(6.6x)
B. animalis
(2.5x)
L. acidophilus
(3.7x)
F. prausnitzii
(3.5x)
C. difficile
(6.2x)
B. vulgatus
(3.2x)
3.5x
R. intestinalis
(5.8x)
R. obeum
(4.3x)
S. aureus
(10x)
C. albicans
(6.2x)
M. tuberculosis
(32.5x)
SEB
(0.6x)
CD154+ (%)
CD154+ of naive T cells (CD45RA+)
CD154+ of memory T cells (CD45RA-)
B
Memory (%)
S. typhimurium
C. difficile
Total CD4 T cells
C
Memory CD4 T cells
(live CD3+ CD4+ CD154+ CD45RA-)
TNF-α (%)
IL-2 (%)
S. typhimurium
E. coli
B. animalis
L. acidophilus
F. prausnitzii
C. difficile
B. vulgatus
R. intestinalis
R. obeum
S. aureus
M. tuberculosis
C. albicans
D
CD4+ CD154+ CD45RA- T cells
CD4+ CD154- CD45RA- T cells
B. animalis stimulation
CCR6
Integrin β7
CCR9
CCR2
CCR4
CCR7
CCR10
CXCR3
CXCR5
CD161

**Supplementary Figure 2.** Detection and characterization of microbiota-specific memory $CD4^+$ T cells (related to Figure 1 and 2). (*A*) Frequencies of $CD154^+$ cells among naïve and memory peripheral $CD4^+$ T cells in adults after short-term stimulation with heat-inactivated bacteria. *Dots* represent different donors (n = 30). (*B*) Percentage of memory cells within $CD4^+CD154^+$ T cells. Each *symbol* represents an antigen-reactive population from 1 individual; the *line* indicates the mean of experiments performed independently with blood obtained at different times (n = 19−30). Significance calculated in relation to total $CD4^+$ T cells. (*C*) Percentages of cytokine-expressing cells among memory $CD4^+CD45RA^-CD154^+$ T cells are shown. Frequencies (±SEM) of 27 independent donors are depicted. (*D*) Surface marker and chemokine receptor expression frequencies among $CD4^+$ $CD45RA^-$ $CD154^+$ and $CD4^+$ $CD45RA^-$ $CD154^-$ T cells after short-term stimulation with *B animalis*. Frequencies within $CD4^+$ $CD45RA^-CD154^+$ or $CD4^+$ $CD45RA^-$ $CD154^-$ T cells are depicted. Statistics: (*A*) Mann-Whitney tests; (*B*) 1-way analysis of variance with Sidak's multiple comparison test; ns, not significant; $^*P \leq .05$; $^{**}P \leq .01$; $^{***}P \leq .001$; $^{****}P \leq .0001$.

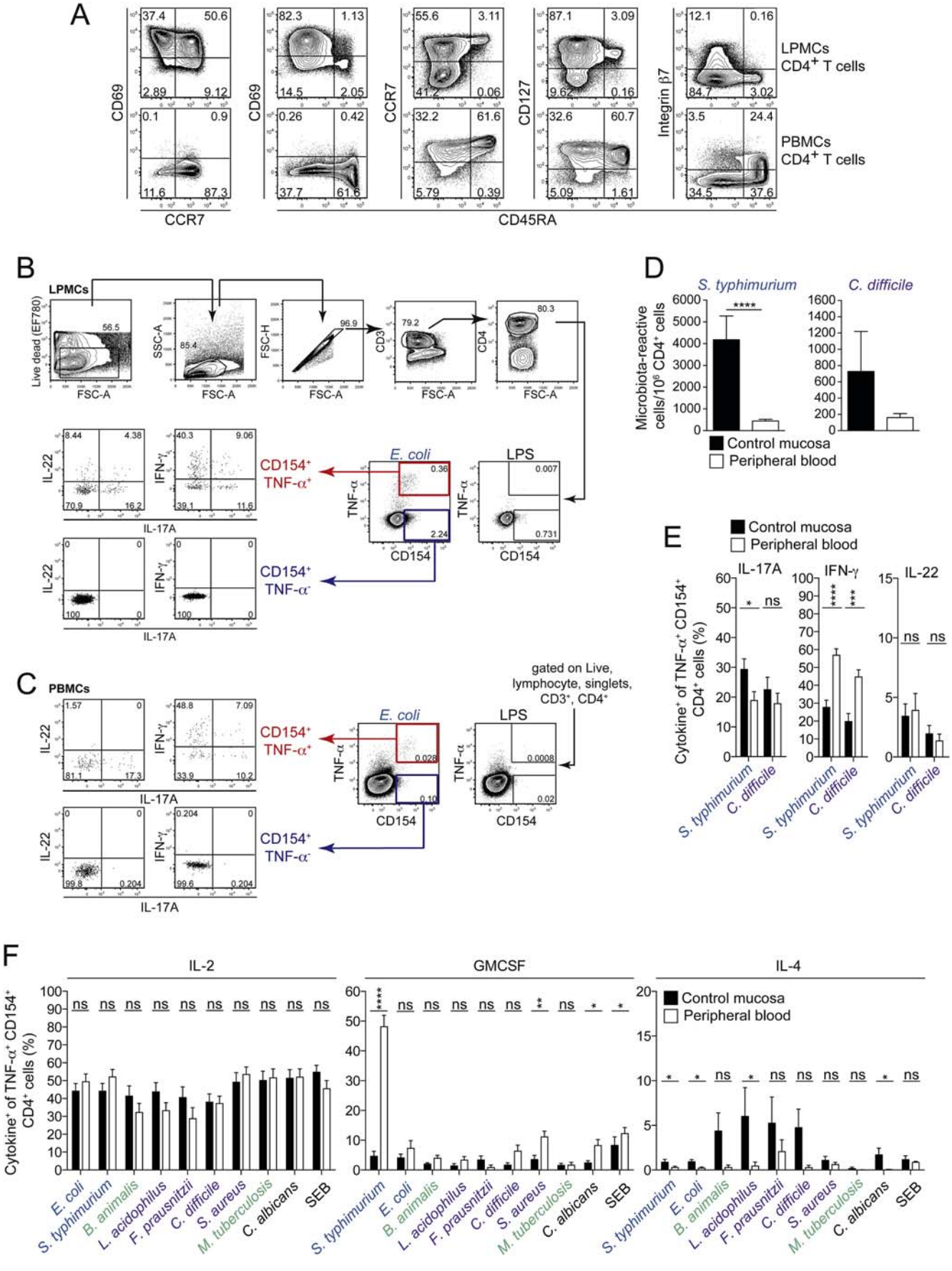
A
CD69
CCR7
CD45RA
CD127
Integrin β7
LPMCs
CD4+ T cells
PBMCs
CD4+ T cells
B
LPMCs
Live dead (EF780)
SSC-A
FSC-H
CD3
CD4
FSC-A
IL-22
IFN-γ
IL-17A
TNF-α
CD154
E. coli
LPS
CD154+
TNF-α+
CD154+
TNF-α-
C
PBMCs
gated on Live, lymphocyte, singlets, CD3+, CD4+
D
S. typhimurium
C. difficile
Microbiota-reactive cells/10^6 CD4+ cells
****
Control mucosa
Peripheral blood
E
Control mucosa
Peripheral blood
IL-17A
IFN-γ
IL-22
Cytokine+ of TNF-α+ CD154+ CD4+ cells (%)
ns
S. typhimurium
C. difficile
F
IL-2
GMCSF
IL-4
Cytokine+ of TNF-α+ CD154+ CD4+ cells (%)
Control mucosa
Peripheral blood
E. coli
S. typhimurium
B. animalis
L. acidophilus
F. prausnitzii
C. difficile
S. aureus
M. tuberculosis
C. albicans
SEB

**Supplementary Figure 3.** Detection and characterization of microbiota-specific $CD4^+$ T cells within gut-resident memory T cells (related to Figure 3). (*A*) Representative flow cytometry plots showing CD45RA, integrin $\beta7$, CD69, CCR7, and CD127 expression in gut-resident $CD3^+CD4^+$ T cells. Data representative of 10 independent donors. (*B*, *C*) Gating strategy for identification of enteric bacteria-specific memory $CD4^+$ T cells in lamina propria mononuclear cell (LPMCs) and PBMCs after stimulation with heat-inactivated *E coli* in a representative donor. (*D*) LPMCs were stimulated with heat-inactivated bacteria and analyzed for CD154 expression. Estimated gut resident microbiota-reactive cells per million $CD4^+$ T cells compared with adult blood is depicted ($n = 17$ for control mucosa; $n = 25-31$ for blood). (*E*, *F*) Cytokine production by $CD4^+CD154^+$TNF-$\alpha^+$ T cells after short-term stimulation with the indicated heat-inactivated bacteria. Frequencies (±SEM) of 10−23 independent donors. Significance calculated between the respective stimulations in control mucosa and peripheral blood. Statistics: (*D*, *E*, *F*) Mann-Whitney test; ns, not significant; $^*P \leq .05$; $^{**}P \leq .01$; $^{***}P \leq .001$; $^{****}P \leq .0001$.

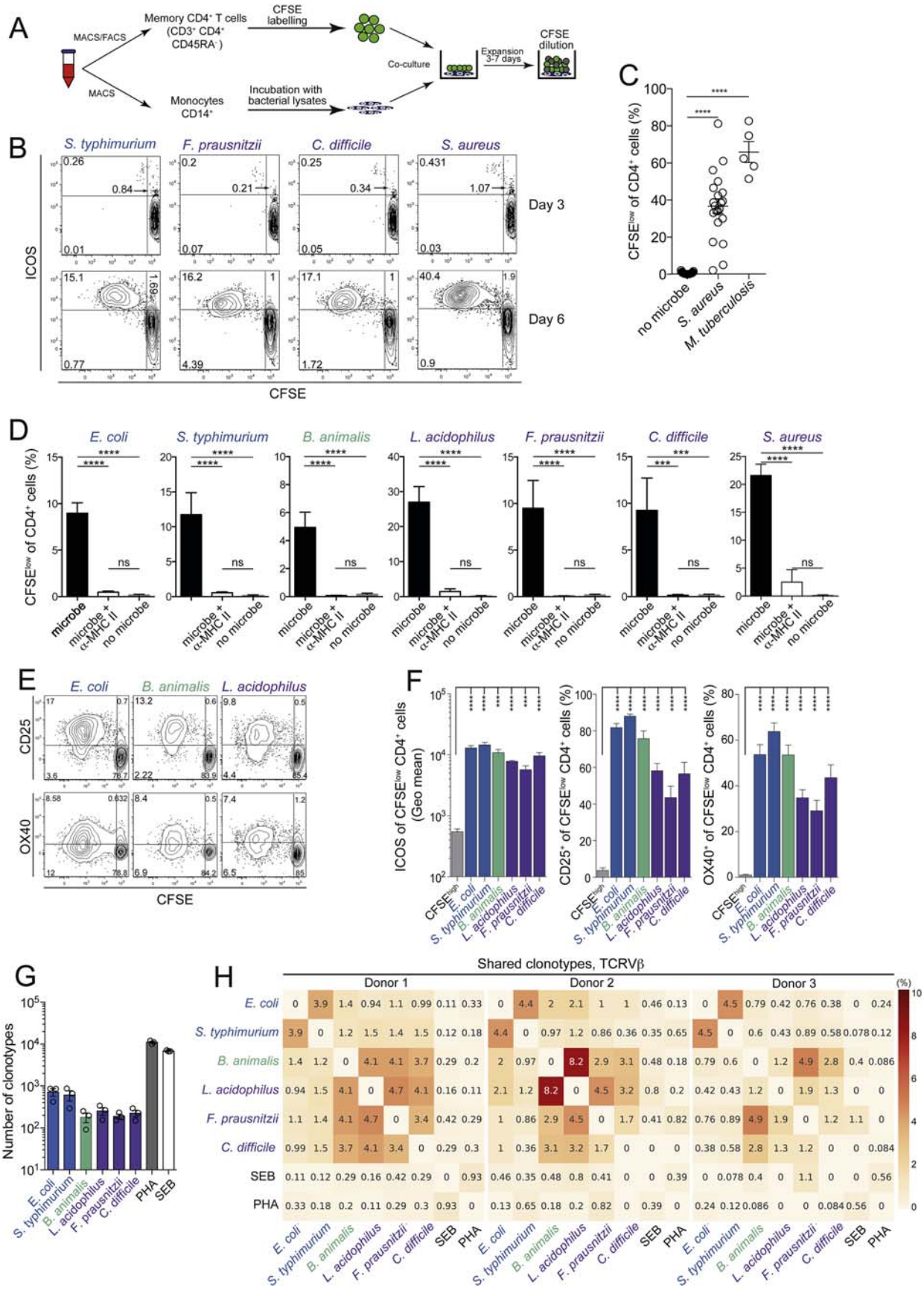
A
MACS/FACS
Memory CD4+ T cells (CD3+ CD4+ CD45RA-)
CFSE labelling
MACS
Monocytes CD14+
Incubation with bacterial lysates
Co-culture
Expansion 3-7 days
CFSE dilution
B
S. typhimurium
F. prausnitzii
C. difficile
S. aureus
Day 3
Day 6
ICOS
CFSE
C
CFSElow of CD4+ cells (%)
no microbe
S. aureus
M. tuberculosis
D
E. coli
S. typhimurium
B. animalis
L. acidophilus
F. prausnitzii
C. difficile
S. aureus
CFSElow of CD4+ cells (%)
microbe
microbe + α-MHC II
no microbe
ns
E
E. coli
B. animalis
L. acidophilus
CD25
OX40
CFSE
F
ICOS of CFSElow CD4+ cells (Geo mean)
CD25+ of CFSElow CD4+ cells (%)
OX40+ of CFSElow CD4+ cells (%)
CFSEhigh
E. coli
S. typhimurium
B. animalis
L. acidophilus
F. prausnitzii
C. difficile
G
Number of clonotypes
E. coli
S. typhimurium
B. animalis
L. acidophilus
F. prausnitzii
C. difficile
PHA
SEB
H
Shared clonotypes, TCRVβ
Donor 1
Donor 2
Donor 3
(%)
E. coli
S. typhimurium
B. animalis
L. acidophilus
F. prausnitzii
C. difficile
SEB
PHA

**Supplementary Figure 4.** Expansion and detection of microbiota-specific memory $CD4^+$ T cells (related to Figure 4). Total memory $CD4^+$ T cells were isolated, labeled with CFSE, and cultured with autologous irradiated monocytes in the presence or absence of the indicated heat-inactivated bacteria and blocking antibodies to major histocompatibility complex II (MHCII). (*A*) Experimental setup. (*B*) Shown are the CFSE profiles and ICOS expression on days 3 and 6 of stimulation in a representative donor. (*C*) Frequencies (±SEM) of $CFSE^{low}$ proliferating cells after stimulation with *S aureus* and *M tuberculosis* ($n = 5-21$). Data representative of 5−10 independent experiments. Each *dot* represents an independent donor. (*D*) Frequencies (±SEM) of $CFSE^{low}$ proliferating $CD4^+$ T cells in presence or absence of anti-MHCII. Data representative of 2 independent experiments. (*E, F*) CFSE profiles and expression of CD25 and OX40 on day 6 of stimulation in a representative donor. (*F*) Geometric mean and frequencies (±SEM) of ICOS, CD25, and OX40 expression on $CFSE^{low}CD4^+$ T cells on day 6. (*G*) Number of unique TCR$\beta$ clonotypes detected in bacteria-reactive $CD4^+$ T cells. TCR V$\beta$ sequencing was performed from 3 independent donors. Each *circle* represents an independent donor. TCR V$\beta$ usage of the different reactivities of 3 independent donors is summarized in Supplementary Table 3. (*H*) *Heat map* showing the frequency of shared clonotypes between different bacteria-reactive $CD4^+$ T-cell responses. SEB and phytohemagglutinin (PHA) expanded memory T cells were used as controls. Data from 3 independent donors. The CDR3 sequences are summarized in Supplementary Table 4. Statistics: (*C*, *D*, *F*) 1-way analysis of variance with Sidak's multiple comparison test; ns, not significant; $^*P \leq .05$; $^{**}P \leq .01$; $^{***}P \leq .001$; $^{****}P \leq .0001$.

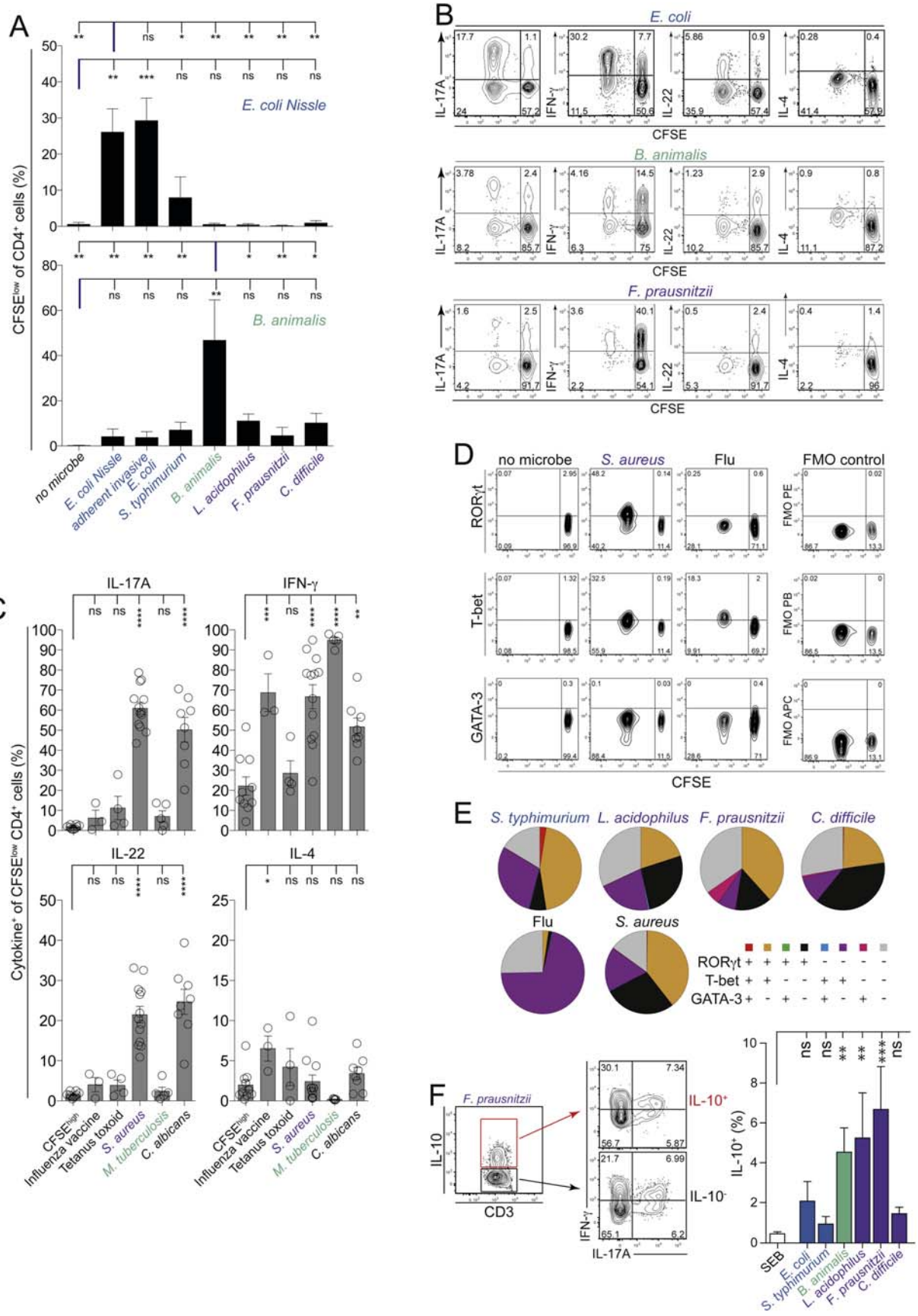
A
E. coli Nissle
B. animalis
CFSE^low of CD4+ cells (%)
no microbe
E. coli Nissle
adherent invasive E. coli
S. typhimurium
B. animalis
L. acidophilus
F. prausnitzii
C. difficile
B
E. coli
B. animalis
F. prausnitzii
IL-17A
IFN-γ
IL-22
IL-4
CFSE
C
IL-17A
IFN-γ
IL-22
IL-4
Cytokine+ of CFSE^low CD4+ cells (%)
CFSE^high
Influenza vaccine
Tetanus toxoid
S. aureus
M. tuberculosis
C. albicans
D
no microbe
S. aureus
Flu
FMO control
RORγt
T-bet
GATA-3
FMO PE
FMO PB
FMO APC
CFSE
E
S. typhimurium
L. acidophilus
F. prausnitzii
C. difficile
Flu
S. aureus
RORγt
T-bet
GATA-3
F
F. prausnitzii
IL-10
CD3
IL-10+
IL-10-
IFN-γ
IL-17A
IL-10+ (%)
SEB
E. coli
S. typhimurium
B. animalis
L. acidophilus
F. prausnitzii
C. difficile

**Supplementary Figure 5.** Cross-reactivity, cytokine production, and transcription factor expression by antigen-reactive memory $CD4^+$ T cells (related to Figure 5). (*A*) $CD154^+$ memory CD4 T cells from PBMCs were sorted after short-term stimulation with *E coli* and *B animalis* lysates and expanded them for 10−14 days with CD3/CD28 and IL2. The *E coli Nissle*- and *B animalis*−reactive T cell lines were CFSE-labeled and then co-incubated with autologous monocytes loaded with the various bacterial lysates. Frequencies (±SEM) of $CFSE^{low}$ proliferating cells after 5 days of stimulation with the indicated bacteria are shown. Data from 3−6 independent donors. (*B*−*F*) Total memory $CD4^+$ T cells were isolated, labeled with CFSE and cultured with autologous irradiated monocytes in the presence of the indicated heat-inactivated bacteria or antigens. (*B*, *C*) Production of cytokines by proliferating $CFSE^{low}$ cells measured by intracellular staining after phorbol myristate acetate (PMA)/ionomycin stimulation on day 7 of primary stimulation with monocytes and heat-inactivated bacteria. Frequencies (±SEM) of 3−13 independent donors are depicted. Each *dot* represents an independent donor. (*D*, *E*) Related orphan receptor γt (RORγt), T-box expressed in T cells (T-bet), and GATA-binding factor-3 (GATA-3) expression on day 7 of primary stimulation with monocytes and influenza seasonal vaccination or heat-inactivated *S aureus* in a representative donor. (*E*) Boolean gating analysis showing each possible combination of RORγt, T-bet, and GATA-3 production by $CFSE^{low}$ proliferating cells. Data generated from 3 independent donors. (*F*) Production of IL10 by expanded $CFSE^{low}$ $CD4^+$ cells after PMA/ionomycin stimulation. Frequencies (±SEM) and IFN-gamma/IL17A co-expression within $IL10^+$ and $IL10^-$ cells are depicted from 5−8 independent donors. Statistics: (*A, C*) 1-way analysis of variance with Sidak's multiple comparison test; (*F*) Kruskal-Wallis test with Dunn's multiple comparison; ns, not significant; ***$P \leq .001$; ****$P \leq .0001$.

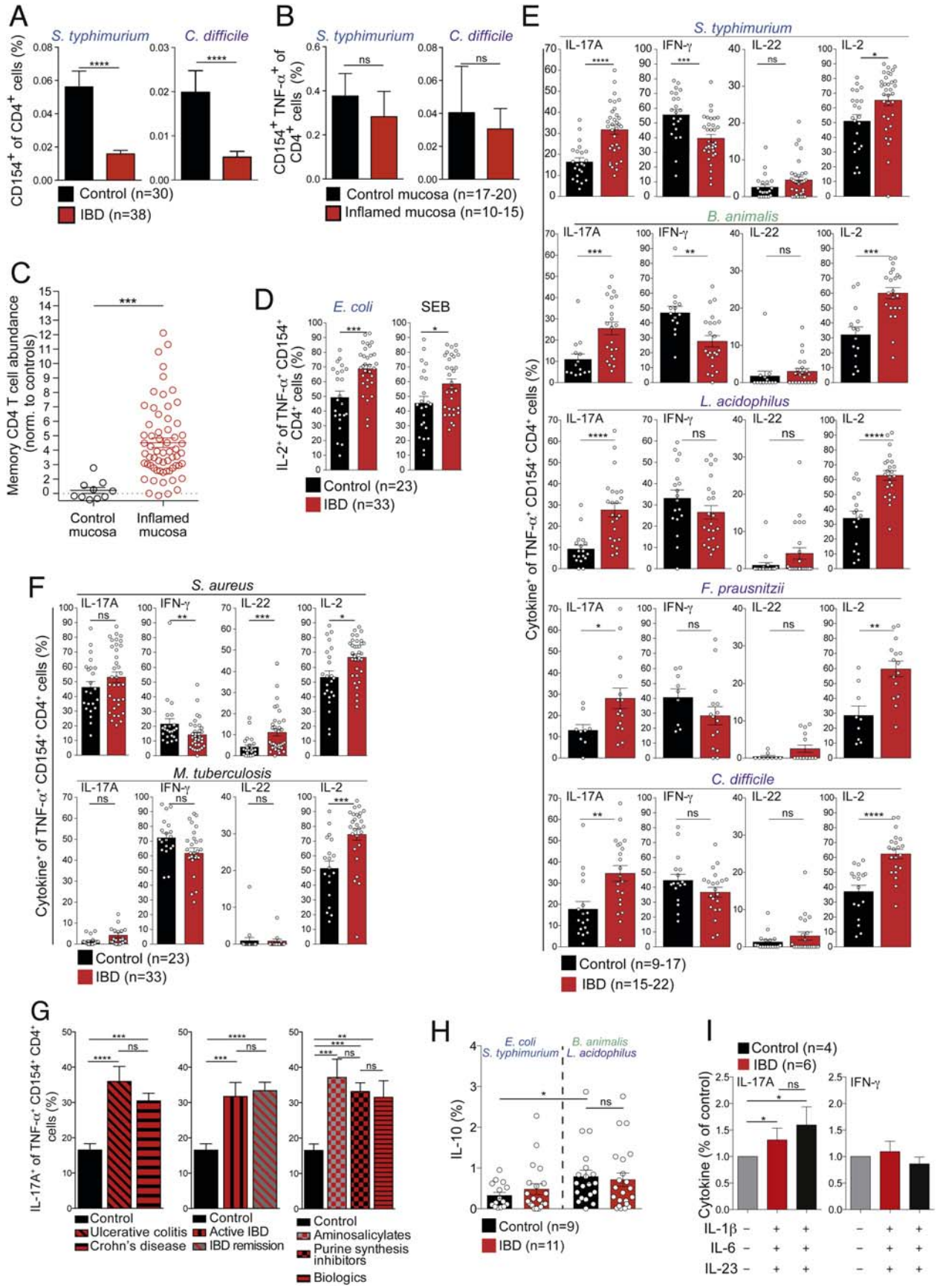
A
S. typhimurium
C. difficile
CD154+ of CD4+ cells (%)
Control (n=30)
IBD (n=38)
B
S. typhimurium
C. difficile
CD154+ TNF-α+ of CD4+ cells (%)
Control mucosa (n=17-20)
Inflamed mucosa (n=10-15)
C
Memory CD4 T cell abundance (norm. to controls)
Control mucosa
Inflamed mucosa
D
E. coli
SEB
IL-2+ of TNF-α+ CD154+ CD4+ cells (%)
Control (n=23)
IBD (n=33)
E
S. typhimurium
B. animalis
L. acidophilus
F. prausnitzii
C. difficile
IL-17A
IFN-γ
IL-22
IL-2
Cytokine+ of TNF-α+ CD154+ CD4+ cells (%)
Control (n=9-17)
IBD (n=15-22)
F
S. aureus
M. tuberculosis
IL-17A
IFN-γ
IL-22
IL-2
Cytokine+ of TNF-α+ CD154+ CD4+ cells (%)
Control (n=23)
IBD (n=33)
G
IL-17A+ of TNF-α+ CD154+ CD4+ cells (%)
Control
Ulcerative colitis
Crohn's disease
Control
Active IBD
IBD remission
Control
Aminosalicylates
Purine synthesis inhibitors
Biologics
H
E. coli
S. typhimurium
B. animalis
L. acidophilus
IL-10 (%)
Control (n=9)
IBD (n=11)
I
Control (n=4)
IBD (n=6)
IL-17A
IFN-γ
Cytokine (% of control)
IL-1β
IL-6
IL-23

**Supplementary Figure 6.** Functional characteristics of enteric bacteria-reactive $CD4^+$ T cells in IBD (related to Figure 7). (*A*) PBMCs isolated from healthy donors or IBD patients were stimulated with the indicated heat-inactivated bacteria and analyzed for CD154 expression. Frequencies (±SEM) of reactive $CD154^+$ cells among $CD4^+$ T cells in peripheral blood are depicted (n = 30−38). Demographic and clinical characteristics of IBD patients are summarized in Supplementary Table 6. (*B*) Lamina propria mononuclear cell (LPMCs) were isolated from inflamed surgical specimens from IBD patients or non-inflamed and tumor-free surgical specimens from colorectal cancer patients. Isolated LPMCs were stimulated with the indicated heat-inactivated bacteria and analyzed for CD154 expression. Frequencies (±SEM) of reactive $CD154^+$ TNF-$\alpha^+$ cells among $CD4^+$ T cells in peripheral blood are depicted (n = 10−20). (*C*) Microarray analysis of intestinal biopsies obtained at endoscopy (n = 6 controls, 24 ulcerative colitis (UC) and 37 Crohn's disease (CD); Gene Expression Omnibus entry GSE16879). The relative abundance of memory $CD4^+$ T cells in control and inflamed IBD tissue was estimated in silico using CIBERSORT (see Supplementary Methods for details). (*D*−*F*) PBMCs isolated from healthy and IBD patients were stimulated with the indicated heat-inactivated bacteria or SEB and analyzed for CD154 expression and intracellular cytokine expression. Demographic and clinical characteristics of IBD patients are summarized in Supplementary Table 6. (*D*) IL2 expression in $CD154^+$ TNF-$\alpha^+$ memory $CD4^+$ T cells after stimulation with the indicated heat-inactivated bacteria or SEB. Frequencies (±SEM) of 23-33 independent donors. Each dot represent an independent donor. (*E, F*) IL17A, IFN-gamma, IL22, and IL2 expression in $CD154^+$ TNF-$\alpha^+$ memory $CD4^+$ T cells after stimulation with the indicated heat-inactivated bacteria. Each *dot* represents an independent donor. Demographic and clinical characteristics of IBD patients are summarized in Supplementary Table 6. (*G*) IL17A expression in $CD154^+$ TNF-$\alpha^+$ memory $CD4^+$ T cells after stimulation with *S typhimurium*. IBD patients were categorized by disease phenotype (UC, CD), disease activity according to clinical notes, and current treatment. (*H*) Total memory $CD4^+$ T cells were isolated from healthy controls or IBD patients blood, labeled with CFSE and cultured with autologous irradiated monocytes in the presence of the indicated heat-inactivated bacteria or antigens. Production of IL10 by expanded $CFSE^{low}$ $CD4^+$ cells after phorbol myristate acetate (PMA)/ionomycin stimulation on day 7 of stimulation. Frequencies (±SEM) are depicted from 9−11 independent donors. (*I*) $CD4^+CD45RO^+CD45RA^-CD25^-CD8^-$ memory $CD4^+$ T cells were isolated from healthy controls or IBD patients blood, labeled with CFSE, and stimulated with autologous monocytes pulsed with *B animalis* in the presence or absence of the indicated cytokines. Data represent mean (±SEM) fold changes in IL17A or IFN-gamma expression frequencies relative to cells expanded without cytokines. Statistics: (*A*−*E, G*−*H*) Mann-Whitney test; (*F*) 1-way analysis of variance with Sidak's multiple comparison test; ns, not significant; $^*P \leq .05$; $^{**}P \leq 0.01$; $^{***}P \leq .001$; $^{****}P \leq .0001$.

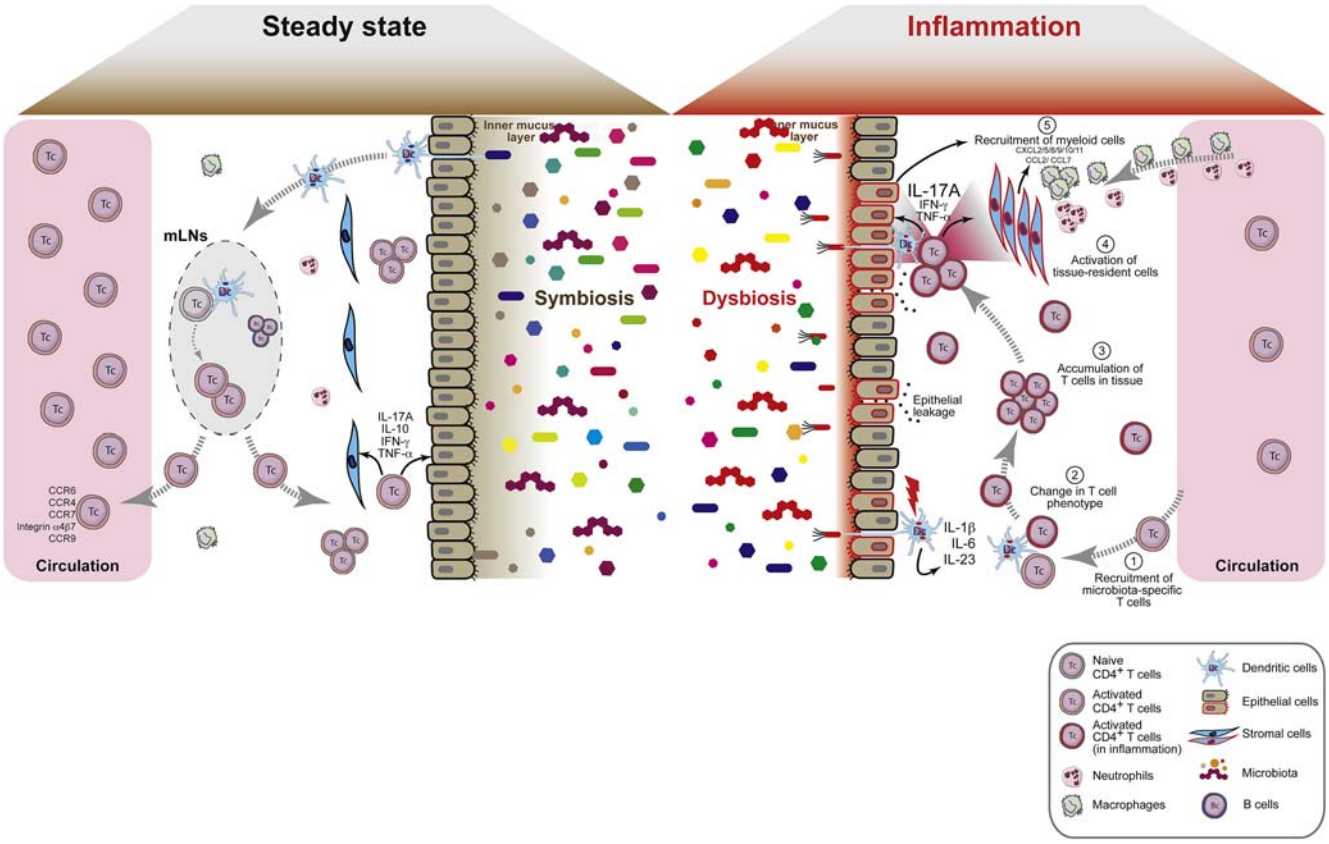


**Supplementary Figure 7.** Microbiota-specific memory T-cell responses in intestinal homeostasis and inflammation. Microbiota-specific memory $CD4^+$ T cells are abundant in peripheral blood and mucosa. Luminal sampling of intestinal microbiota by dendritic cells and repetitive epithelial breaches after birth might induce $CD4^+$ T-cell responses targeted towards intestinal bacteria. Enteric bacteria-specific $CD4^+$ T cells produce barrier-protective cytokines, such as IL17A, IFN-gamma, and IL22. Furthermore, certain commensal-specific $CD4^+$ T cells also produce IL10. We speculate that the cytokine production by commensal-specific $CD4^+$ T cells might play a significant role in supporting gut homeostasis and the mutualistic relationship with intestinal microbiota. In inflammation, epithelial break down and leakage leads to increased availability of luminal antigens and bacterial stimuli, which activate the innate system and the expression of Th17-inducing cytokines (IL1$\beta$, IL6, and IL23). Recruited microbiota-specific memory $CD4^+$ T cells accumulate in inflamed mucosa and are polarized toward more IL17A production. Activated memory cells express IL17A, TNF-$\alpha$, and IFN-gamma, which stimulate intestinal cells, such as stromal and epithelial cells, to express various chemokine ligands and cytokines. This may promote recruitment and activation of myeloid cell populations.